PATENT
Attorney Docket 062614-5001

IN THE UNITED STATES PATENT AND TRADEMARK OFFICE

In re Patent of: **Yong YAO *et al.***	)	
Application No. **10/087,217**	)	Examiner: **John D. ULM**
Filed: **March 4, 2002**	)	Group Art Unit: **1646**
For: **NOVEL CELL-BASED ASSAYS FOR G-PROTEIN COUPLED RECEPTOR MEDIATED ACTIVITIES**	)	

DECLARATION UNDER 37 C.F.R. 1.132

I, Xiao Li, do hereby make the following declaration:

1. As shown by my attached cv, I have served as Manager and Principal Scientist of Assay Development at BD Biosciences since 2004. I have seven years of research and development experience developing screening assays in the biomedical and biotechnology industries. From 2002 to 2004, I was a Senior Application Scientist for Molecular Devices Corporation; from 1999 to 2001, I was a staff scientist at Invitrogen Corporation; and from 1998 to 1999, I was a postdoctoral scientist at Life Technologies, Inc. I earned a B.S. in Genetics and Genetics Engineering from Fudan University in Shanghai, a M.S. in Molecular Biology from the University of Rochester, and a Ph.D. in Molecular Biology from the University of Rochester.

2. I have read and understand the Office Action that was mailed June 13, 2005, in the above-referenced application, including the rejection under 35 U.S.C. § 112, first paragraph. It is my understanding that the basis for the rejection is that the specification does not disclose the use of a negative control to identify activity of a specific exogenous (non-native) G protein-coupled receptor (GPCR), to the exclusion of endogenous GPCRs. Further, it is my understanding that the Office Action asserts that a comparative step that

employs a cell that is otherwise identical to the test cell but for the presence of the GPCR of interest is critical to the practice of the invention.

3. In response, it is my expert opinion that any scientist working in the fields of molecular biology and protein interactions is well aware that it is routine to include appropriate controls in any scientific experiment. In particular, it was well known at the time this application was filed that assays to detect activity of exogenous GPCRs may include the use of controls to account for endogenous GPCR activity, as would be commonly used in any biological assay measuring the activity of a transfected, exogenous protein. Furthermore, it was well known in the art that a negative control for GPCR expression is not always necessary, for instance where the host cell is known not to express relevant endogenous GPCRs.

4. This declaration summarizes references which were publicly available prior to the filing of the above-referenced application and which are relevant to my conclusion that a scientist practicing in this field would have known when to use a control as part of the claimed invention and would have known what controls should be used.

5. Glucagon-like peptide 2 receptor (GLP-2R) is a member of the parathyroid hormone receptor-like G Protein-Coupled Receptor B family. Glucagon-like peptide 2 (GLP-2) is a ligand of GLP-2R. Munroe *et al.* published the results of a cAMP assay in 1990 in which COS cells were transiently transfected with a GLP-2R expression construct in order to assess whether a predicted GLP-2R sequence encoded a functional receptor (see page 1572, column 1, first full paragraph of Munroe *et al.*, *Proc. Natl. Acad. Sci. USA.*, 96: 1569-1573, 1990). As Figure 2(A) illustrates, untreated cells, vector only cells (*i.e.*, no GLP-2R expression), cells treated with Forskolin (an activator of the cAMP pathway), and cells expressing various other polypeptides were used as controls in the assay to compare to the response of the GLP-2R transfected cells exposed to GLP-2.

6. Lee *et al.* published data in 1998 which suggests that sphingosine-1-phosphate is a ligand for G protein-coupled receptor EDG-1 and that overexpression of EDG-1 induces exaggerated cell-cell aggregation (see Lee *et al.*, *Science*, 279: 1552-1555, 1998). HEK293 cells were transfected with human EDG-1 cDNA in an expression vector or transfected with an expression vector only as a negative control (see page 1552, column 2). Figure 2(a) on page 1553 shows the results of an aggregation assay which includes a vector control as well as a EDG-1 only control (*i.e.*, no added activator or inhibitor).

7. A 1999 publication authored by Nothacker *et al.* describes how an orphan G protein-coupled receptor referred to as GPR14 was identified as a receptor for mammalian urotensin II (see Nothacker *et al.*, *Nature Cell Biol.*, 1: 383-385, 1999). In order to identify the ligand of GPR14, peptide extracts from a variety of mammalian tissues were fractionated by preparative reverse-phase high-performance liquid chromotography, and aliquots were tested for induction of change in intracellular Ca^{2+} in Chinese hamster ovary cells (CHO) transiently transfected with GPR14 cDNA, non-transfected CHO cells, and control CHO cells transfected with other orphan receptors (see page 383, second paragraph). A reproducible change in Ca^{2+} concentration was observed in two adjacent fractions containing urotensin II for the cells transfected with GPR14 cDNA but not for the control cells.

8. Apoptosis can be mediated by activation of a G protein-coupled receptor for parathryoid hormone (PTH) and parathyroid hormone-related protein (PTHrP). The G protein-coupled receptor, referred to as PTHR, is capable of signaling in response to PTH or PTHrP through the activation of phospholipase C resulting in increased Ca^{2+} and through the activation of adenylyl cyclase resulting in cAMP production. In 2000, Turner *et al.* published the results of experiments conducted to determine whether activation of phospholipase C and/or activation of adenylyl cyclase are responsible for

triggering apoptosis in HEK293 cells (see Turner *et al.*, *Mol. Endo.*, 14: 241-254, 2000). The HEK293 cells used in the experiments were engineered to express wild-type opossum PTHR while lacking endogenous PTHR, therefore negating the need for a negative GPCR control (page 242, column 1, lines 31-33). Figure 6(B) provides the results of an apoptosis assay in which the control consists of HEK293 cells expressing opossum PTHR without the addition of activators and inhibitors.

9. In summary, having reviewed the above-referenced application and the pending claims, it is my expert opinion that any scientist practicing in this field would know how to routinely use appropriate controls in any scientific method. Furthermore, given the references discussed above, which are exemplary of the field of GPCR expression prior to October 26, 2001 (the priority date of the subject application), a scientist working in this field would know when and how to include the use of one or more controls in the method of the instant invention. As described in the references above, it was well known that the control for a cell transfected with a GPCR expression vector can be an identical cell transfected with only the expression vector or a non-transfected cell. It was also known that a negative control is not necessary, however, if the cell expressing the exogenous GPCR is void of endogenous GPCR.

10. I further declare that all statements made herein of my own knowledge are true, and that all statements made on information and belief are believed to be true, and further, that these statements were made with the knowledge that willful false statements and the like so made are punishable by fine or imprisonment, or both, under Section 1001 of Title 18 of the United States Code, and that such willful false statements may jeopardize the validity of the application or any patent issuing thereon.

Oct 13, 2005
Date

Xiao Li, Ph.D.

XIAO LI

Home Address	17826 Fairlady Way, Germantown, MD 20874
Telephone	240-888-6049
E-mail	xiao_li@bd.com

EDUCATION

1993-1997	Ph. D. Molecular Biology, University of Rochester, Rochester, NY 14627
1991-1993	Master of Science, Molecular Biology, University of Rochester, Rochester, NY 14627
1987-1991	Bachelor of Science, Genetics and Genetic Engineering, Fudan University, Shanghai, P. R. China.

PROFESSIONAL EXPERIENCE

2004 to current

Manager & Principal Scientist of Assay Development, Bioimaging Systems R&D, BD Biosciences.

Projects: Managing the assay development team to develop assays for high throughput GRCR and ion channel screenings. Designing and develop assays for BD's high content analysis platform.

- Lead the assay development team to develop assays for drug discovery:
  1. Optimize the ACT*One* assay, the only high-throughput GPCR screening technology to directly measure the intracellular concentration of the secondary messenger cAMP in living cells, in real-time.
  2. Further develop the ACT*One* assay for deorphanizing receptors and monitoring endogenous receptor activities in both cell lines and primary cells.
  3. Provide consultation to ACT*One* users in high throughput screening labs in pharmaceutical and biotech companies.
  4. Develop, manufacture and QC the ACT*One* cell lines that stably express GPCRs for high throughput screenings.
  5. Develop, manufacture and QC proprietary assay kits to for high throughput GPCR and ion channel screenings.
  6. Collaborate with other sites within the organization to apply the in-house technologies to the bioimaging platform for developing high content analysis applications.

- Participate in evaluating new technologies and collaborating with other companies in cell analysis field. Lead one of the evaluation projects and one of the collaboration projects across the sites in BD Biosciences.
- Participate in the strategic planning team for designing next generation instrumentations and assay platforms in cell analysis field.
- Present seminar on the ACT*One* technology in pharmaceutical companies. Train technical support groups at different sites in BD Biosciences.

2002 to 2004

Senior Application Scientist for Molecular Devices Corporation, a major instrumentation and assay platform supplier for high throughput screening society.

Projects: Worked with high throughput screening labs in pharmaceutical and biotech companies to develop assays with Molecular Devices' instruments for high throughput screenings.

- Provided consultation and support to scientists in assay development and high throughput screening labs. Developed and trouble shot the following assays:
  1. Cell based assay for GPCR screening: FLIPR assay, cAMP assays, SPA binding assay, BRET assay and reporter gene assays.
  2. Cell based assay for ion channel screening: membrane potential measurements and automated patch clamp.
  3. Biochemical assays for kinase, phosphatase and phosphodiesterase screening: IMAP assay, HTRF assay, DEFIA assay and Elisa based assays.

- Demonstrated and trained customers on drug discovery instruments and softwares. The instruments include:
  1. FLIPR, the industrial standard instrument for cell-based high throughput GPCR and ion channel screenings.
  2. FlexStation, a medium throughput instrument mainly for assay development of a FLIPR assay.
  3. CLIPR, a microplate imager for high throughput screening of luminescence and SPA assays.
  4. Analyst, a multimode PMT based plate (96, 384, 1536 well plates) reader to read fluorescence intensity, fluorescence polarization, time resolve fluorescence, absorbance and luminescence.
  5. Discovery 1, an integrated system for cell based high content screening applications.
  6. IonWorks HT, an automated patch clamp instrument that dramatically increases the throughput of Ion-channel screening and drug safety testing (hERG channel activity).

- Studied various screening platforms, analyzed pros and cons of each method, identified emerging technologies, and wrote technical and marketing reports to the product development teams.

- Trained new application scientists.

1999 – 2001	Staff Scientist, Invitrogen Corporation. Projects: Specialized in developing tools for functional genomics and proteomics fields. • Developed the yeast reverse two-hybrid system, a powerful tool to screen for specific compound or proteins that interfere with protein-protein interactions. • Developed a new version of the yeast forward two-hybrid system compatible with Invitrogen's flagship product, the Gateway Cloning System. • Wrote large sections of the manual for the yeast two-hybrid system kit. • Developed the Gateway Cloning System cDNA library transfer kit. • Involved in developing high throughput protein expression platform. • Provided consultation and technical support to internal and external customers. • Provided training and technical lectures for coworkers, customers and collaborators. • Set up yeast Two-Hybrid screening service labs at the company headquarter and the division in Japan, and applied automations to increase the throughput. • Initiated and coordinated collaborations with several academic labs to develop new technologies.
1998 – 1999	Postdoctoral Scientist, Life Technologies Inc. Project: • Developing the yeast reverse two-hybrid system.
1997 - 1998	Howard Hughes Research Associate at Duke University. Research Project: • Studied the mechanism of how rapamycin, an immunosuppressive antifungal product, affects translation efficiency of multiple genes and interferes with the signal transduction pathways.
1991 - 1997	Graduate Research Assistant at Department of Biology at University of Rochester. Research Projects: • Studied structure and function relationship *of E. coli* ribosomal protein L4. • Cloned the *Bacillus subtilis* ribosomal protein S10 operon, and analyzed transcriptional and translational regulation mechanisms of this 15kb cluster. • Studied the ribosomal RNA processing pathways, especially the processing of ITS-I (intragenic transcribed spacer I) region, in yeast *Saccharomyces cerevisiae*.
1989 - 1991	Undergraduate Research Assistant at the Institute of Genetics, Fudan University. Research Projects: • Subcloned and expressed human interleukin-2 receptor (IL-2R) gene in Chinese Hamster Ovary (CHO) cell line.

- Examined the importance of the 3'-untranslated region of the IL-2R mRNA by deletion analysis.

OTHER PROFESSIONAL EXPERIENCES

1992	Teaching Assistant for Cell Biology, University of Rochester
1993	Teaching Assistant for Genetics, University of Rochester
1999	Reviewer for scientific journal Gene

AWARDS

1997 – 1998	Howard Hughes Medical Institute Research Associate Fellowship
1988 – 1991	Academic Excellence Scholarship, Fudan University
1984 - 1987	Valedictorian of the High School Affiliated with East China Normal University, Shanghai, China

PUBLICATIONS

1. Zengel, J. M., D. Vorozheikina, X. Li, and L. Lindahl. (1995) Regulation of the *Escherichia coli* S10 ribosomal protein operon by heterologous L4 ribosomal proteins. Biochemistry and Cell Biology, 73:1105-1112.

2. Li, X., L. Lindahl and J. M. Zengel. (1996) Ribosomal protein L4 from *Escherichia coli* utilizes nonidentical determinants for its structural and regulatory functions. RNA, 2:24-37.

3. Li, X., L. Lindahl, Y. Sha and J. M. Zengel. (1997) Analysis of the *Bacillus subtilis* S10 ribosomal protein gene cluster identifies two promoters that may be responsible for transcription of the entire 15-kilobase S10-spc-alpha cluster. J. Bacterial. 179 22: 7046-7054.

4. Yan Zhang, Evelyn McGown, Michael Su, Luke Lavis and Xiao Li. (2003) Optimization of measurement parameters and performance comparison for Analyst GT and Analyst HT or Acquest. Poster at ScreenTech World Summit 2003.

5. Jianming Lu, Isabel Llorente, Yong Yao, Paul lee and Xiao Li (2004) Analysis of Gi-coupled receptors with BD ACT*One* technology. Poster at Assay & Cellular Targets meeting 2004.

REFERENCES

Upon request.

Proc. Natl. Acad. Sci. USA
Vol. 96, pp. 1569–1573, February 1999
Medical Sciences

Prototypic G protein-coupled receptor for the intestinotrophic factor glucagon-like peptide 2

DONALD G. MUNROE*†, ASHWANI K. GUPTA*, FATEMEH KOOSHESH*, TEJAL B. VYAS*, GEIHAN RIZKALLA*, HONG WANG*, LIDIA DEMCHYSHYN*, ZHI-JIE YANG*, RAJENDER K. KAMBOJ*, HONGYUN CHEN*, KIRK MCCALLUM*, MARTIN SUMNER-SMITH*‡, DANIEL J. DRUCKER§, AND ANNA CRIVICI*¶

*Allelix Biopharmaceuticals Inc., 6850 Goreway Drive, Mississauga, Ontario L4V 1V7, Canada; and §Department of Medicine, The Toronto Hospital, Banting and Best Diabetes Centre, University of Toronto, Toronto, Ontario M5G 2C4, Canada

Edited by Donald F. Steiner, The University of Chicago, Chicago, IL, and approved November 18, 1998 (received for review August 18, 1998)

ABSTRACT **Glucagon-like peptide 2 (GLP-2) is a 33-aa proglucagon-derived peptide produced by intestinal enteroendocrine cells. GLP-2 stimulates intestinal growth and upregulates villus height in the small intestine, concomitant with increased crypt cell proliferation and decreased enterocyte apoptosis. Moreover, GLP-2 prevents intestinal hypoplasia resulting from total parenteral nutrition. However, the mechanism underlying these actions has remained unclear. Here we report the cloning and characterization of cDNAs encoding rat and human GLP-2 receptors (GLP-2R), a G protein-coupled receptor superfamily member expressed in the gut and closely related to the glucagon and GLP-1 receptors. The human GLP-2R gene maps to chromosome 17p13.3. Cells expressing the GLP-2R responded to GLP-2, but not GLP-1 or related peptides, with increased cAMP production (EC_{50} = 0.58 nM) and displayed saturable high-affinity radioligand binding (K_d = 0.57 nM), which could be displaced by synthetic rat GLP-2 (K_i = 0.06 nM). GLP-2 analogs that activated GLP-2R signal transduction *in vitro* displayed intestinotrophic activity *in vivo*. These results strongly suggest that GLP-2, like glucagon and GLP-1, exerts its actions through a distinct and specific novel receptor expressed in its principal target tissue, the gastrointestinal tract.**

Glucagon-like peptides (GLPs) encoded by the proglucagon gene play key roles in glucose homeostasis, gastric emptying, insulin secretion, and appetite regulation (1). Glucagon and GLP-1 exert their effects through distinct G protein-coupled receptors (GPCRs). In contrast, unique receptors for GLP-2, glicentin, and oxyntomodulin have not yet been identified, despite considerable attempts at receptor isolation via classical molecular biology approaches (2). Recent studies have shown that GLP-2 is a potent intestinal growth factor that stimulates crypt cell proliferation and inhibits epithelial apoptosis (3). GLP-2 promotes epithelial proliferation in both small and large intestine; however, the mechanisms utilized by GLP-2 for promotion of intestinal growth remain unclear.

To understand the mechanisms underlying GLP-2 action, we have carried out studies directed at the identification and cloning of the putative GLP-2 receptor. We now have isolated rat and human cDNAs encoding GLP-2-responsive GPCRs, which show highest similarity to receptors for glucagon and GLP-1. The GLP-2R is coupled to activation of adenylate cyclase, and the receptor is expressed selectively in rat hypothalamus and the gastrointestinal tract, known targets of GLP-2 action. These findings establish GLP-2 as a novel hormone that, like glucagon and GLP-1, exerts its actions through a distinct receptor expressed in a highly tissue-restricted manner. The GLP-2R should provide an important target for isolation of small molecules mimicking GLP-2 action and for future studies delineating specific mechanisms underlying GLP-2 action in the gut and central nervous system.

The publication costs of this article were defrayed in part by page charge payment. This article must therefore be hereby marked "*advertisement*" in accordance with 18 U.S.C. §1734 solely to indicate this fact.

PNAS is available online at www.pnas.org.

Methods and Materials

Primers, cDNA Libraries, and Cloning Strategy. Initial attempts at low-stringency hybridization of intestine and brain cDNA libraries using GLP-1R/GlucagonR cDNA sequences were not successful. Two million cDNA clones from rat hypothalamus and rat duodenum/jejunum cDNA libraries subsequently were screened with degenerate oligonucleotides derived from conserved transmembrane II and VII GPCR coding sequences: C4–4 (5′-AACTACATCCACMKGM AYCTGTTYVYGTCBTTCATSCT-3′) (IUB nomenclature) and C9–2R (5′-TCYRNCTGSACCTCMYYRTTGAS-RAARCAGTA-3′) (for nomenclature, see ref. 4). First-round cDNA plugs (1,057) were isolated in this screen. In a complementary strategy, PCR was conducted on intestinal cDNA templates by using sets of degenerate PCR primers, based on conserved transmembrane amino acid motifs from family B GPCRs or from motifs conserved mainly within the glucagon/glucose-dependent insulinotropic polypeptide (GIP)/GLP-1 receptor subfamily. PCR products were Southern-blotted and probed with ^{32}P-end-labeled C4–4 oligonucleotide. PCRs, amplified from rat neonatal intestine cDNA (Stratagene; catalog no. 936508) were chosen for cloning. These products had been amplified with the degenerate primers M2F (5′-TTTTTCTAGAASRTSATSTACACNGT SGGCTAC-3′) (based on conserved transmembrane domain I sequences) and M7R (5′-TTTTCTCGAGCCARCARCCASSWRTART-TGGC-3′) (based on conserved transmembrane III sequences). PCR products were cloned into pBluescript, screened by filter hybridization with the nested C4-4 oligonucleotide, and sequenced, leading to the identification of a sequence fragment from a novel GPCR family B member, designated WBR, that ultimately proved to be the GLP-2R. Two new GLP-2R-specific PCR primers, P23-F1 (5′-TCTGACAGATATGA-CATCCATCCAC-3′) and P23-R1 (5′-TCATCTCCCTCT-TCTTGGCTCTTAC-3′), were used to screen the 1,057 cDNA plugs obtained by hybridization screening, leading to the

This paper was submitted directly (Track II) to the *Proceedings* office.
Abbreviations: EBNA, Epstein–Barr nuclear antigen; GPCR, G protein-coupled receptor; GLP-1 and -2, glucagon-like peptide 1 and 2, respectively; GLP-2R, GLP-2 receptor; GIP, glucose-dependent insulinotropic polypeptide.
Data deposition: The sequences reported in this paper have been deposited in the GenBank database (accession nos. AF105367 and AF105368).

†To whom reprint requests should be addressed. e-mail: dmunroe@allelix.com.
‡Present address: Base4 Bioinformatics, 6299 Airport Road, Mississauga, Ontario L4V 1N3, Canada.
¶Present address: Ligard Pharmaceuticals, Inc. 10275 Science Center Drive, San Diego, CA 92121.

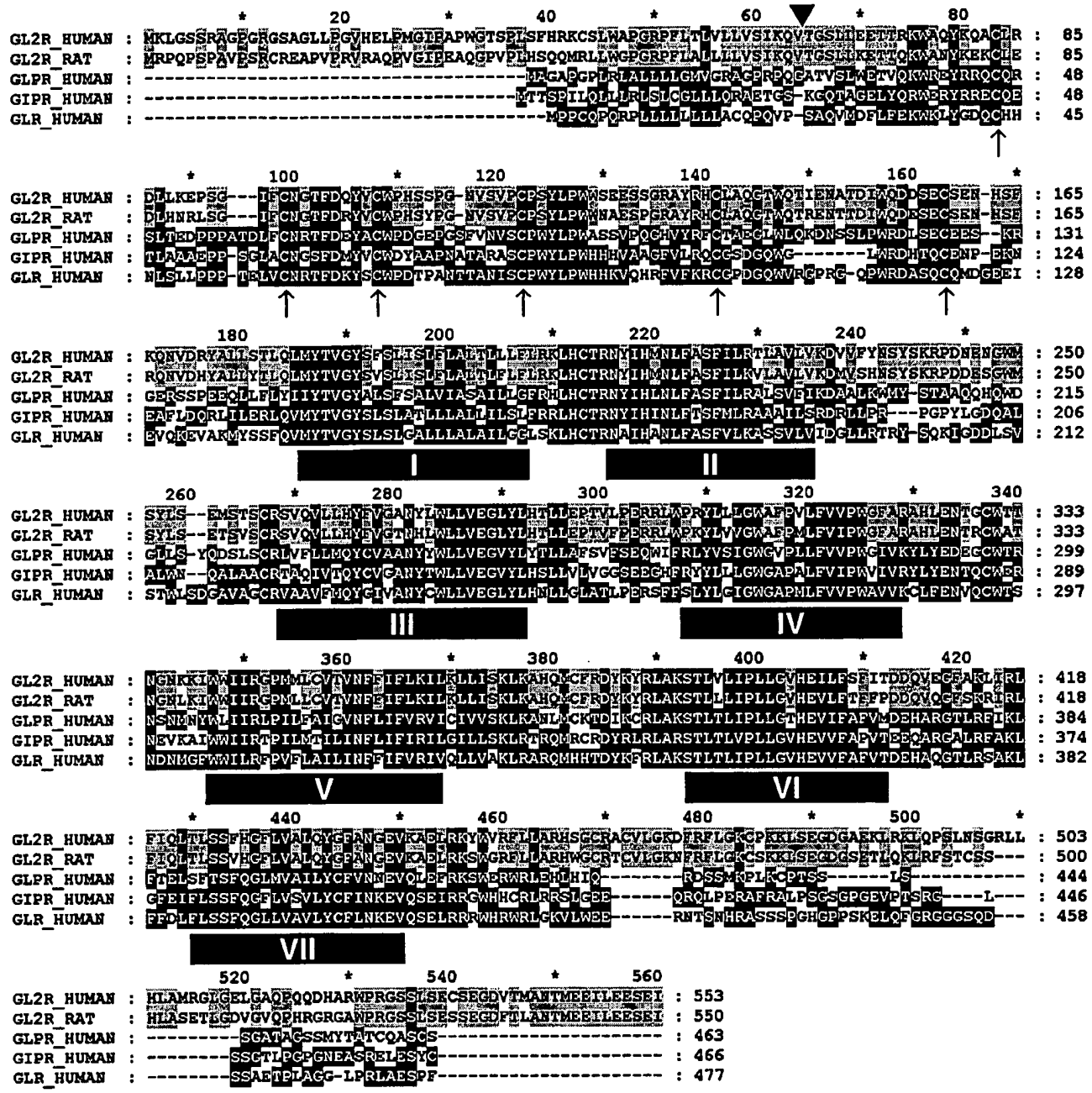

FIG. 1. Multiple alignment of the human (GL2R_HUMAN) and rat (GL2R_RAT) GLP-2R amino acid sequences with human GLP-1, GIP, and glucagon receptor sequences. Known receptor sequences are designated by Swiss-Prot identifiers. Alignment was performed with CLUSTAL W 1.60 and rendered with GENEDOC 2.2. Identities of rat and human GLP-2R sequences is shown in gray, and identities across all five receptor members are indicated by black shading. A predicted signal-peptide cleavage site in human and rat GLP-2R is indicated by an inverted triangle. Six conserved cysteine residues are indicated by arrows. Seven predicted transmembrane domains are shown as solid, black boxes labeled with Roman numerals, and asterisks are shown for spacing every 20 aa. The GenBank accession numbers for the human and rat GLP-2R sequences are AF105367 and AF105368, respectively.

identification of three independent clones, two from the duodenum/jejunum library and a third from hypothalamus, which, together, contained a 2,537-bp cDNA insert encoding full-length rat GLP-2R.

To clone the human GLP-2R, the coding region of the rat GLP-2R was used to screen a human hypothalamus cDNA library (CLONTECH; catalog no. 1172a), from which a single positive clone (HHT13) was isolated and sequenced. A full-length insert was ligated into pcDNA3 for expression studies.

Intestinotrophic Activity, cAMP Determination, and Radioligand-Binding Studies. For cAMP assays, an episomal stable cell line was prepared by lipofection of 293-EBNA (Epstein–Barr nuclear antigen) cells (Invitrogen) with a pREP7-based (Invitrogen) construct containing the Met-42 → Ile-550 ORF of rGLP-2R. Parental 293-EBNA cells, as well as the stable cell line rG2R, expressed receptors for vasoactive intestinal polypeptide and pituitary adenylate cyclase-activating polypeptide. Therefore, the ligand specificity of GLP-2R was tested further in transiently transfected COS cells, which expressed no functional receptors for any of the ligands tested.

For cAMP assays, cells were treated at 80% confluency with GLP-2 peptide analogs at concentrations ranging from 10^{-12}

to 10^{-5} M for 30 min in medium containing 3-isobutylmethylxanthine. The reaction was terminated with the addition of 95% ethanol and 5 mM EDTA. Aliquots of the ethanol extract were used to determine cAMP levels using an enzyme immunoassay kit (Amersham) as described by the manufacturer. Results were analyzed with GRAPHPAD PRISM software and expressed as pmol cAMP per well. For radioligand-binding assays, cells expressing GLP-2R were harvested and homogenized in 25 mM Hepes (pH 7.4) buffer containing 140 mM NaCl, 0.9 mM $MgCl_2$, 5 mM KCl, 1.8 mM $CaCl_2$, 17 mg/ml Diprotin A, and 100 μM phenanthroline. Homogenates were centrifuged for 10 min at 1,000 × *g* at 4°C to remove cellular debris. For saturation experiments, membranes containing 25 μg protein were incubated with increasing concentrations of ^{125}I-[Tyr-34]GLP-2 (5–2,000 pM final concentration) in a volume of 0.5 ml for 2 hr at 4°C. Nonspecific binding was determined by the addition of 10 μM of native rat GLP-2 and subtracted from total binding to estimate specific binding to GLP-2R. Parallel experiments confirmed the lack of specific binding when the GLP-2R expression construct was not used. For competition-binding experiments, assays were initiated by the addition of 200 pM (final concentration) of ^{125}I-[Tyr34]GLP-2 with increasing concentrations of competing peptide analogs (10^{-11} to 10^{-5} M) for 2 hr as described above. Reactions were terminated by centrifugation at 13,000 × *g* for 15 min at 4°C. The pellets were washed three times with cold 50 mM Tris buffer, and radioactivity was quantitated in a gamma counter. Results were analyzed by GRAPHPAD PRISM software.

Intestinotrophic activities of various peptide analogs were determined by assessment of small bowel weight as described (5), after 14-day treatments with 2.5 μg of test peptide or PBS (vehicle-treated control) administered twice daily. Activity was defined as follows: active, small bowel wet weight 40–70% greater than in vehicle-treated control animals; partially active, 20–40% greater than controls; inactive, less than 20% greater than controls.

RNAse Protection Assay. A fragment of GLP-2R cDNA was subcloned into pBluescript (Stratagene) for *in vitro* transcription with T3 or T7 RNA polymerases. The probe, called F1, spanned nucleotides encoding amino acids Met-1 → Arg-210. RNase protection assay was carried out essentially as described (6), using 50 μg of total RNA from adult rat tissues or 50 μg of yeast tRNA (negative control) or tRNA spiked with a known copy number of sense-strand cRNA (for standard curve construction). Each sample was hybridized with 100,000 cpm of [^{32}P]CTP-labeled antisense cRNA and then digested with RNases T1 (140 units/ml) and A (8 μg/ml) at 30 C for 1 hr. The deproteinized, ethanol-precipitated probe was run on a 5% sequencing gel and analyzed after PhosphorImaging (Molecular Dynamics) with IMAGEQUANT software. RNA copy number was calculated by interpolation relative to the standard curve after taking the lengths and specific activities of undigested and digested probes into account. A second RNase probe from a different region of the GLP-2R cDNA was used to confirm the quantitative results (data not shown).

RESULTS AND DISCUSSION

GLP-2 and the peptide hormones GLP-1, glucagon, and GIP have closely related amino acid sequences (7). Similarly, the sequences of cloned receptors for the latter three peptides form a cluster within the parathyroid hormone receptor-like GPCRs family B (8–11), suggesting that the GLP-2 receptor might also be found within this subfamily. Initial attempts at GLP-2 receptor cloning by conventional screening of cDNA libraries at low stringency with a combination of GLP-1 and glucagon receptor cDNA probes were not successful. Accordingly, we next used a combined approach of reverse transcription–PCR and hybridization screening followed by expression

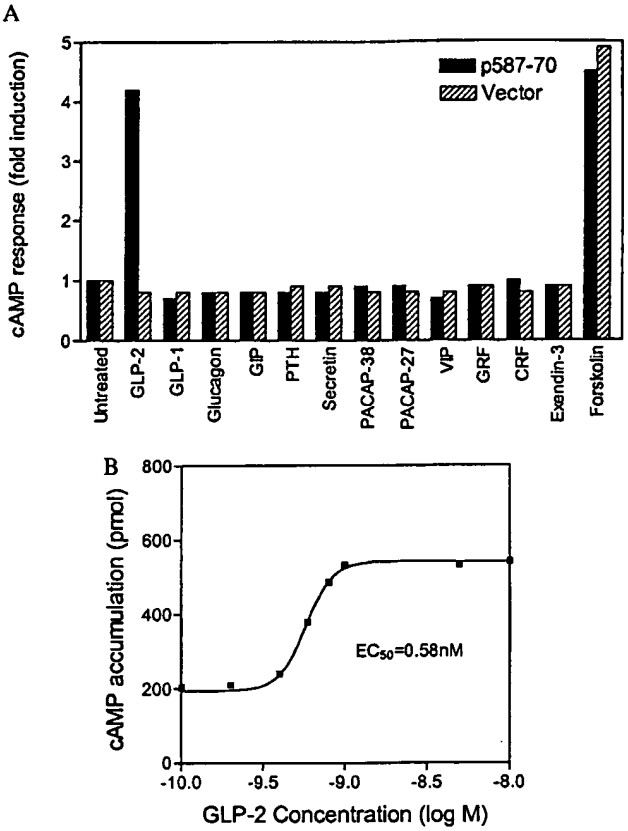

FIG. 2. Ligand-selective and concentration-dependent cAMP response to rat GLP-2 in transiently lipofected COS cells. (*A*) Ligand specificity of cAMP response to GLP-2. cAMP response to peptide analogs of family 2 GPCR ligands was determined in COS cells transiently lipofected with the GLP-2R expression vector p587-70 or the parental pcDNA3 expression vector. GLP-2 concentration was 1 nM; all other peptides were used at 10 nM. A similar profile of peptide specificity was observed with the human GLP-2R (data not shown). (*B*) Concentration–response curve for cAMP accumulation in response to synthetic rat GLP-2 in rG2R cells stably expressing GLP-2R.

analysis of candidate cDNAs. As described in *Methods and Materials*, this strategy resulted in the isolation of a 2,537-bp rat GLP-2R cDNA insert encoding a 550-aa putative family B GPCR (Fig. 1). Hydropathy analysis of the GLP-2R amino acid sequence revealed a typical 7-transmembrane topology plus a hydrophobic amino-terminal signal peptide (data not shown). The GLP-2R gene product belongs to the GLP-1/glucagon/GIP receptor gene subfamily. Conserved features include a possible signal-peptide cleavage site between Val-64 and Thr-65, potential *N*-glycosylation sites within the amino-terminal putative extracellular domain, and six cysteine residues conserved in the mature GLP-1, GIP, and glucagon receptor amino-terminal domains (Fig. 1). Two putative alternative translation initiation codons, Met-1 and Met-42, were found amino-terminal to the first transmembrane domain in the rat GLP-2R. Functional analysis of Met-1 and Met-42 site-directed mutants showed they were functionally identical (unpublished results), consistent with signal-peptide removal predicted to yield an identical 486-aa mature polypeptide. Overlapping regions of the hypothalamus and duodenum/jejunum cDNA clones encoded homologous polypeptide fragments. Moreover, no evidence was obtained for differential splicing of intestinal GLP-2R RNA from an RNase protection assay employing two nonoverlapping probes derived from GLP-2R cDNA, which together spanned 387 of the 550 GLP-2R codons (data not shown). Additionally, sequencing of

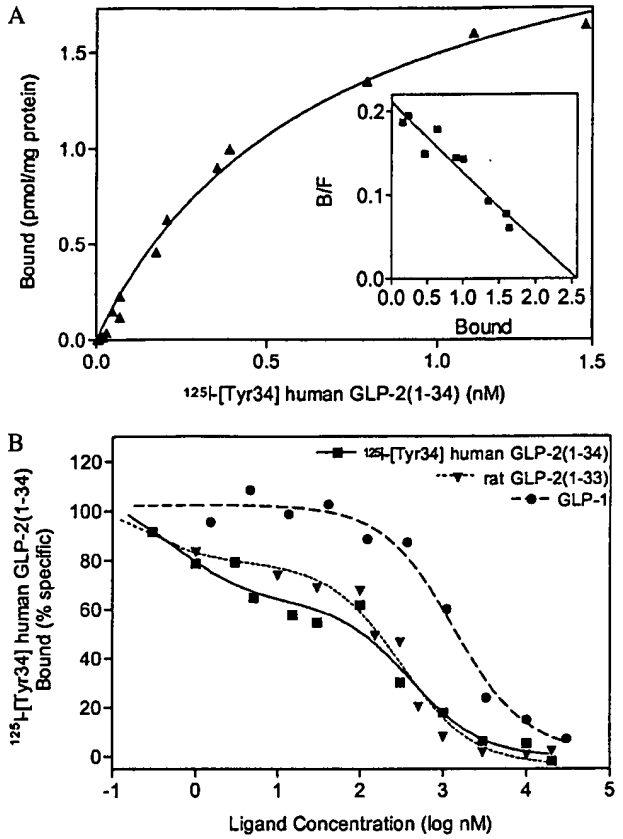

FIG. 3. Binding of ^{125}I-[Tyr-34]GLP-2 to cell membranes prepared from rG2R cells stably transfected with GLP-2R cDNA. (*A*) Saturation isotherms of the specific binding of ^{125}I-[Tyr-34]GLP-2 to membranes. Results shown are representative of six independent experiments, each conducted in triplicate. From Scatchard analysis (*Inset*), maximal-binding B_{max} was estimated at 1,839 fmol/mg protein, and a K_d value of 0.57 nM was obtained. (*B*) Competition binding of ^{125}I-[Tyr-34]GLP-2 binding to cell membranes in the presence of unlabeled peptides. Data are shown for the concentration-dependent inhibition of ^{125}I-[Tyr-34]GLP-2 binding (200 pmol) to GLP-2R by various peptide analogs from at least two independent experiments conducted in triplicate. Inhibitory constants (K_i) were estimated by using GRAPHPAD PRISM.

the full-length human GLP-2R cDNAs confirmed the identity of hypothalamic and gastrointestinal GLP-2Rs (Fig. 1).

To assess whether the predicted GLP-2R sequence encodes a functional GLP-2 receptor, a GLP-2R expression construct, p587-70, was transiently transfected into COS cells. Because related family B GPCRs show functional coupling to cAMP production mediated by the heterotrimeric G protein Gs, cAMP accumulation was measured after incubation with GLP-2. Treatment of GLP-2R-transfected COS cells with 1 nM GLP-2 resulted in a 4-fold rise in cAMP levels relative to untreated cells, approximately equal to the response seen with 10 μM forskolin (Fig. 2*A*). Treatment with 10 nM GLP-1, glucagon, GIP, exendin-3, and seven other family B GPCR ligands did not induce cAMP production in p587-70-transfected cells. Control cells transfected with vector DNA alone failed to respond to any of the peptides tested, including GLP-2, though forskolin did induce cAMP production.

With a stable GLP-2R episomal expression cell line, rG2R, greater than 20-fold cAMP induction routinely was achieved with 1 or 10 nM GLP-2 (data not shown), confirming the potent induction of cAMP accumulation by GLP-2. In contrast, the nontransfected 293-EBNA cells showed no response to GLP-2. The EC_{50} of the cAMP response to GLP-2 in rG2R cells was 0.58 nM (Fig. 2*B*). The presence of saturable, specific, ligand-selective GLP-2-binding sites on these cells was shown by using a radioiodinated, C-terminally extended GLP-2 analog, ^{125}I-[Tyr-34]GLP-2 (Fig. 3*A*). From Scatchard analysis of the saturation isotherms, a B_{max} value of 1,839 fmol/mg of protein and a K_d of 0.57 nM were obtained for the radioligand. Mock-transfected cells showed no specific binding to the radioligand (data not shown). Competition-binding studies with rat GLP-2 revealed a high-affinity site (K_i = 0.06 nM) and a low-affinity site (K_i = 259 nM) (Fig. 3*B*). In contrast, no high-affinity GLP-1 sites were observed in the transfected GLP-2R/rG2R clone. K_i values determined for GLP-1, glucagon, and GIP peptides were 928, 500, and 765 nM, respectively. Although the binding and Scatchard data may reflect, in part, a degree of receptor overexpression, the functional studies and binding data provide firm evidence for a cDNA that encodes a functional high-affinity, ligand-selective GLP-2 receptor.

The human GLP-2R polypeptide showed 81.6% similarity to rat GLP-2R (Fig. 1). Functional expression of the cloned human GLP-2R conferred a functional response to GLP-2 and the appearance of high-affinity ligand-binding sites on 293-EBNA cells, similar to data obtained with the rat GLP-2R (data not shown). Furthermore, the cloned human GLP-2 receptor exhibited the same profile of peptide-binding specificity (Fig. 2*A* and unpublished data) as the rat receptor. The gene encoding human GLP-2R was identified by screening an arrayed BAC library of human genomic DNA (Genome Systems, St. Louis), confirmed by sequencing, and mapped to chromosome 17p13.3 by fluorescence *in situ* hybridization analysis (data not shown).

A quantitative ribonuclease protection assay method was used to determine the tissue distribution of rat GLP-2R RNA because no signals were detected on multitissue Northern blots. GLP-2R RNA levels were highest in jejunum, followed by duodenum, ileum, colon, and stomach, whereas expression was undetectable in seven other tissues (Table 1). This expression pattern is clearly concordant with previously reported functional responses to GLP-2 in duodenum (12, 13), jejunum, ileum (5, 12, 14, 15), and colon (12, 16, 17); in contrast, no proliferative or histological changes were seen after GLP-2 treatment in spleen, heart, kidney, lung, or brain (18). Thus, GLP-2R expression is detected in known GLP-2 target tissues. This observation, together with the functional data from

Table 1. Quantitative GLP-2R RNA distribution in various rat tissues determined by RNase protection

Tissue	F1 quantitation, copies per μg total RNA	β-Actin quantitation, copies per μg total RNA	GLP-2R/-actin, ratio
Jejunum	11,900	15,500,000	76.8×10^{-5}
Duodenum	9,150	85,700,000	10.7×10^{-5}
Ileum	7,490	51,400,000	14.6×10^{-5}
Colon	4,150	19,800,000	21.0×10^{-5}
Stomach	1,530	23,600,000	6.48×10^{-5}
Brain	<600	40,600,000	$<1.48 \times 10^{-5}$
Heart	<600	6,600,000	$<9.09 \times 10^{-5}$
Kidney	<600	14,900,000	$<4.03 \times 10^{-5}$
Liver	<600	16,700,000	$<3.59 \times 10^{-5}$
Lung	<600	38,500,000	$<1.56 \times 10^{-5}$
Muscle	<600	4,600,000	$<13.0 \times 10^{-5}$
Spleen	<600	44,800,000	$<1.34 \times 10^{-5}$

Total RNA (50 μg) from rat tissues or sense-strand cRNA standards was hybridized to radiolabeled antisense cRNA probes prepared *in vitro* from GLP-2R cDNA (F1) or actin cDNA. After RNase digestion as described in *Methods and Materials*, protected probe was precipitated, electrophoresed, and quantitated by PhosphorImage analysis relative to the standard curve obtained from sense-strand cRNA. RNA quantitation is expressed as copy number per μg of total RNA. GLP-2R RNA copy number was detectable to a lower limit of 30,000 copies per 50 μg sample, setting the limit of detection shown above for nongastrointestinal tissues.

Table 2. *In vitro* and *in vivo* activity profiles of selected peptide analogs of GLP-2

Peptide	K_i, nM[a*]		EC_{50}, nM†	E_{max}, %†‡	*In vivo* activity§
	High-affinity	Low-afinity			
rGLP-2(1-33)¶	0.06 ± 0.00	259 ± 46	1.00 ± 0.2	100 ± 0	Active
N-Ac-rGLP-2(1-33)	—	140 ± 2	20.8 ± 0.1	80.1 ± 7	Partially active
[Arg-1]rGLP-2(−1-33)	NA	*n**	901 ± 41	69.0 ± 2	Inactive
[Arg-34]rGLP-2(1-34)	ND	*n*§	3.1 ± 0.3	105 ± 10	Active
[Tyr-34]hGLP-2	0.56 ± 0.3	255 ± 7	1.4 ± 0.1	113 ± 5	Active
rGLP-2(2-33)	—	876 ± 147	210 ± 22	109 ± 8	Inactive
rGLP-2(3-33)	—	251 ± 8	10.7 ± 0.8	115 ± 5	Inactive
rGLP-2(1-29)	0.30 ± 0.00	584 ± 19	3.60 ± 0.4	102 ± 8	Partially active
[Thr-7 insertion]	—	977 ± 470	1,100 ± 30	76 ± 4.0	Inactive
[Gly-2]GLP-2(1-33)	—	126 ± 5	2.0 ± 0.2	103 ± 6	Active
hGLP-2(1-33)¶	1.7 ± 0.4	596 ± 9	1.3 ± 0.20	99 ± 10.6	Active
Glucagon	—	500 ± 332	NA	NA	Inactive
GLP-1(7-36)amide	—	928 ± 1	NA	NA	Inactive
GIP	—	765 (n = 1)	NA	NA	Inactive

NA, not active—no detectable binding; ND, not determined.
*n = 2, except where indicated.
†n = 3.
‡Relative to 100 nM rGLP-2(1-33), n = 3.
§Relative to vehicle-treated control animals, n = 4 or greater. *In vivo* activity is based on changes in small bowel wet weight after 14-day treatment as described in *Methods and Materials*.
¶rGLP-2(1-33) is native rat GLP-2 peptide; hGLP-2(1-33) is native human GLP-2 peptide.

experiments with cloned GLP-2R cDNA, suggests that this receptor mediates the intestinotrophic actions of GLP-2.

Pharmacological support for this hypothesis was obtained from parallel *in vivo/in vitro* studies of GLP-2 analogs containing simple changes in sequence and length (Table 2). Carboxyl-terminal extension analogs bound and activated GLP-2R and retained *in vivo* activity whereas those with amino-terminal extensions lost both activities. Analogs with blocked amino- or carboxyl-terminal residues displayed diminished *in vivo* activity and GLP-2R activation. Insertion of a Thr residue between GLP-2 residues 6 and 7 resulted in loss of activity *in vivo* and *in vitro*. Truncation of the carboxyl-terminus to a 29-residue peptide (analogous to glucagon) reduced but did not eliminate *in vivo* or *in vitro* activities. Interestingly, truncation of one or two amino-terminal residues abolished *in vivo* activity but did not completely eliminate binding or the GLP-2R cAMP response. Taken together, a clear correspondence was revealed between the structural requirements for GLP-2R binding and activation and the *in vivo* intestinotrophic activity of GLP-2, providing additional evidence that the GLP-2R isolated here and the intestinotrophic GLP-2 receptor mediating GLP-2 action *in vivo* are synonymous.

Enteroglucagon synthesis long has been associated with a humoral adaptive response to massive small bowel resection, in which hyperplasia and elongation of jejunal villi are seen (19–22). Proglucagon-derived GLP-2 is detectable in plasma from fasted rats and humans and rises 1.5- to 3.6-fold after feeding (23). Moreover, the intestinotrophic efficacy of GLP-2 has been shown after administration by i.p., i.m., or s.c. routes (14), as well as by coinfusion in parenterally fed rats (12). Thus, it is likely that circulating GLP-2 mediates adaptive changes in the villus-absorptive area in the small intestine. The cloning and characterization of a GLP-2 receptor expressed in the gastrointestinal tract qualifies GLP-2, like GLP-1, glucagon, and GIP, as a bona fide endocrine hormone and should facilitate the discovery of novel pharmacologic agents with similar functional activity. The expression of GLP-2R in hypothalamus also raises the possibility of as yet undescribed role(s) for this intestinotrophic hormone in the central nervous system.

We thank P. Khanna, Y.-D. Huang, R. Mathieson, Y.-P. Zhang, and E. Fan for technical assistance; and J. W. Dietrich, R. Zastawny, and D. Lee for advice and critical reading of this manuscript. D.J.D. is a consultant to Allelix Biopharmaceuticals Inc.

1. Drucker, D. J. (1998) *Diabetes* **47,** 159–169.
2. McGregor, G. P., Goke, R. & Goke, B. (1998) *Exp. Clin. Endocrinol. Diabetes* **106,** 25–28.
3. Tsai, C.-H., Hill, M., Asa, S. L., Brubaker, P. L. & Drucker, D. J. (1997) *Am. J. Physiol.* **273,** E77–E84.
4. Nomenclature Committee of the International Union of Biochemistry (NC-IUB) (1986) *J. Biol. Chem.* **261,** 13–17.
5. Drucker, D. J., Ehrlich, P., Asa, S. L. & Brubaker, P. L. (1996) *Proc. Natl. Acad. Sci. USA* **93,** 7911–7916.
6. Ausubel, F. M., Brent, R., Kingston, R. E., Moore, D. D., Seidman, J. G., Smith, J. A. & Struhl, K. (1998) *Current Protocols in Molecular Biology* (Wiley, New York).
7. Fehmann, H.-C., Goke, R. & Goke, B. (1995) *Endocrine Rev.* **16,** 390–410.
8. Thorens, B. (1992) *Proc. Natl. Acad. Sci. USA* **89,** 8641–8645.
9. MacNeil, D. J., Occi, J. L., Hey, P. J., Strader, C. D. & Graziano, M. P. (1994) *Biochem. Biophys. Res. Commun.* **198,** 328–334.
10. Jelinek, L. J., Lok, S., Rosenberg, G. B., Smith, R. A., Grant, F. J., Biggs, S., Bensch, P. A., Kuijper, J. L., Sheppard, P. O., Sprecher, C. A., *et al.* (1993) *Science* **259,** 1614–1616.
11. Yasuda, K., Inagaki, N., Yamada, Y., Kubota, A., Seino, S. & Seino, Y. (1994) *Biochem. Biophys. Res. Commun.* **205,** 1556–1562.
12. Chance, W. T., Foley-Nelson, T., Thomas, I. & Balasubramaniam, A. (1997) *Am. J. Physiol.* **273,** G559–G563.
13. Brubaker, P. L., Izzo, A., Hill, M. & Drucker, D. J. (1997) *Am. J. Physiol.* **272,** E1050–E1058.
14. Tsai, C.-H., Hill, M. & Drucker, D. J. (1997) *Am. J. Physiol.* **272,** G662–G668.
15. Cheeseman, C. I. (1997) *Am. J. Physiol.* **273,** R1965–R1971.
16. Drucker, D. J., Deforest, L. & Brubaker, P. L. (1997) *Am. J. Physiol.* **273,** G1252–G1262.
17. Litvak, D. A., Hellmich, M. R., Evers, B. M., Banker, N. A. & Townsend, C. M., Jr. (1998) *J. Gastrointest. Surg.* **2,** 146–150.
18. Tsai, C.-H., Hill, M., Asa, S. L., Brubaker, P. L. & Drucker, D. J. (1997) *Am. J. Physiol.* **273,** E77–E84.
19. Buchan, A. M. J., Griffiths, C. J., Morris, J. F. & Polak, J. M. (1985) *Gastroenterology* **88,** 8–12.
20. Rountree, D. B., Ulshen, M. H., Selub, S., Fuller, C. R., Bloom, S. R., Ghatei, M. A. & Lund, P. K. (1992) *Gastroenterology* **103,** 462–468.
21. Gornacz, G. E., Ghatei, M. A. & Al-Mukthar, M. Y. T. (1984) *Dig. Dis. Sci.* **29,** 1041–1049.
22. Taylor, R. G. & Fuller, P. J. (1994) *Baillieres Clin. Endocrinol. Metab.* **8,** 165–183.
23. Brubaker, P. L., Crivici, A., Izzo, A., Ehrlich, P., Tsai, C.-H. & Drucker, D. J. (1997) *Endocrinology* **138,** 4837–4843.

Sphingosine-1–Phosphate as a Ligand for the G Protein–Coupled Receptor EDG-1

Menq-Jer Lee,* James R. Van Brocklyn,* Shobha Thangada, Catherine H. Liu, Arthur R. Hand, Ramil Menzeleev, Sarah Spiegel,* Timothy Hla*†

The sphingolipid metabolite sphingosine-1–phosphate (SPP) has been implicated as a second messenger in cell proliferation and survival. However, many of its biological effects are due to binding to unidentified receptors on the cell surface. SPP activated the heterotrimeric guanine nucleotide binding protein (G protein)–coupled orphan receptor EDG-1, originally cloned as *Endothelial Differentiation Gene–1*. EDG-1 bound SPP with high affinity (dissociation constant = 8.1 nM) and high specificity. Overexpression of EDG-1 induced exaggerated cell-cell aggregation, enhanced expression of cadherins, and formation of well-developed adherens junctions in a manner dependent on SPP and the small guanine nucleotide binding protein Rho.

Morphogenetic differentiation of cells, a fundamental event in embryonic development, is dysregulated in pathological conditions such as tumorigenesis and angiogenesis. Such differentiation is affected by cell-cell as well as cell-matrix adhesion molecules, which are in turn controlled by extracellular factors (*1*). These processes are regulated by factors that act through G protein–coupled receptors (GPRs) and receptor tyrosine kinases (*2*), as well as by bioactive lipids such as lysophosphatidic acid (LPA), SPP, and sphingosylphosphorylcholine (*3*). Signaling pathways regulated by the small guanine nucleotide binding protein Rho participate in the formation of cadherin-dependent cell-cell contacts (*4*).

The *EDG-1* transcript was cloned as an immediate-early gene induced during differentiation of human endothelial cells into capillary-like tubules, an in vitro model of angiogenesis (*5*). The EDG-1 polypeptide is a prototypical member of an orphan receptor subfamily composed of EDG-2/vzg-1, ARG16/H218, and EDG-3 (*6*, *7*). However, the ligands, physiologically relevant signaling pathways, and function of EDG-1 have not yet been described. We transfected human embryonic kidney 293 fibroblasts (HEK293), which do not express the EDG-1 receptor (*8*), with FLAG epitope–tagged human *EDG-1* cDNA in the *pCDNANeo* expression vector. Several clones expressing EDG-1 (HEK293*EDG-1*) or transfected with vector alone (HEK-293*pCDNA*) were isolated (*9*). All *EDG-1*–expressing clones grown in the presence of fetal bovine serum (FBS) formed a network of cell-cell aggregates (Fig. 1). This morphology resembles the network formation of differentiated endothelial cells. In contrast, vector-transfected cells were evenly distributed and maintained a normal, fibroblast-like morphology. Morphogenesis of HEK293*EDG-1* cells was suppressed by incubation with an antibody that binds to the NH_2-terminal FLAG epitope on the EDG-1 receptor (anti-M2) (Fig. 1). We characterized the factor in serum that synergizes with EDG-1 to induce morphological changes. Heat treatment (95°C, 1 hour) of FBS did not inhibit its effect on morphogenesis of *EDG-1*–transfected cells. However, removal of lipids from FBS by charcoal stripping or by butan-1-ol extraction (*10*) completely removed the factor that caused morphogenesis. Furthermore, the lipids extracted from the charcoal (*10*) induced morphogenetic differentiation in HEK293-*EDG-1* cells (Fig. 1). Thus, the EDG-1 ligand is present in the lipid fraction of serum.

Of serum-borne lipids, only SPP induced EDG-1–dependent morphogenesis, where-

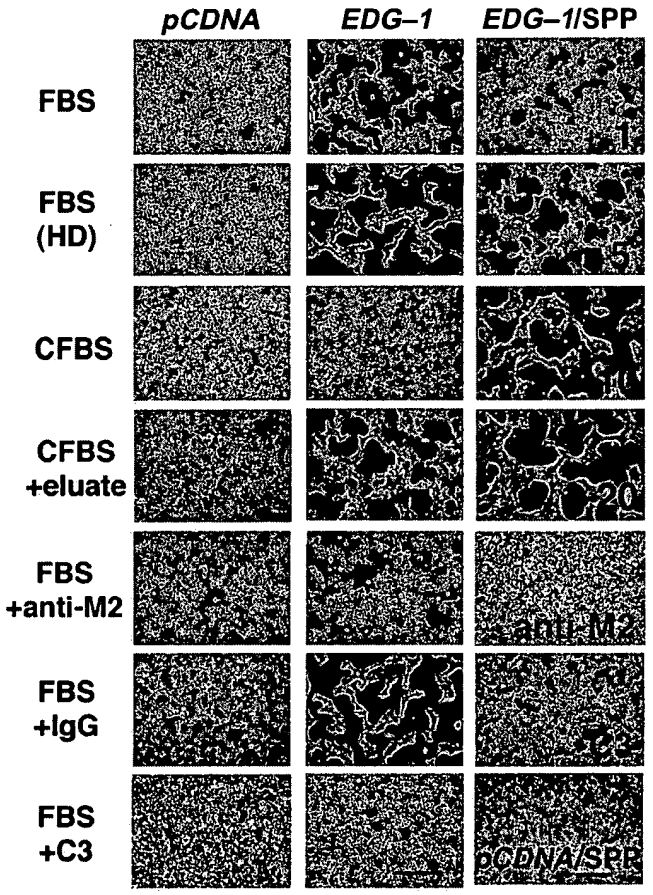

Fig. 1. Presence of a ligand for EDG-1 in the lipid fraction of serum. (**Left**) HEK293*pCDNA* (*pCDNA*) and (**Middle**) HEK293*EDG-1* (*EDG-1*) cells (7.5×10^5 cells/ml) were cultured in six-well plates in Dulbecco's minimum essential medium and 10 mM Hepes (pH 7.4) with the indicated supplements, and cellular morphology was examined after 12 to 15 hours. FBS, 10%; FBS (HD), FBS incubated at 95°C for 1 hour (10%); CFBS, 10%; eluate, serum-derived charcoal-bound lipid eluate (about 120 nmol phospholipid); anti-M2, antibody to FLAG (50 μg/ml; Eastman Kodak); IgG, irrelevant mouse immunoglobulin G (50 μg/ml); C3, C3 exotoxin [cells were pretreated with exotoxin (10 μg/ml) for 2 days; Calbiochem]. Scale bar, 94 μm. (**Right**) EDG-1–dependent morphogenetic differentiation induced by SPP (*EDG-1*/SPP). HEK293-*EDG-1* cells were cultured as described above in medium containing 10% CFBS, and the indicated concentrations of SPP (1, 5, 10, or 20 μM) were added. HEK293*EDG-1* cells were treated with anti-M2 or C3 exotoxin in the presence of 20 μM SPP. *pCDNA*/SPP indicates the effect of 20 μM SPP on HEK293*pCDNA* cells. Scale bar, 56 μm.

M.-J. Lee, S. Thangada, C. H. Liu, T. Hla, Department of Physiology, University of Connecticut School of Medicine, Farmington, CT 06030, USA.
J. R. Van Brocklyn, R. Menzeleev, S. Spiegel, Department of Biochemistry and Molecular Biology, Georgetown University Medical Center, Washington, DC 20007, USA.
A. R. Hand, Department of Pediatric Dentistry, University of Connecticut Health Center, Farmington, CT 06030, USA.

*These authors contributed equally to this work.
†To whom correspondence should be addressed. E-mail: hla@sun.uchc.edu

as sphingosine, sphingomyelin, ceramide, ceramide-1–phosphate, lysophosphatidyl serine, lysophosphatidyl ethanolamine, lysophosphatidyl inositol, lysophosphatidyl choline, leukotriene B4 and C4, platelet-activating factor, anandamide, 12-hydroxyeicosatetraenoic acid (HETE), 15-HETE, and 13-hydroxydodecanoic acid, at concentrations as high as 50 μM, were ineffective. LPA, a bioactive lipid structurally related to SPP, induced morphogenetic differentiation weakly at 20 to 50 μM (*11*). SPP induced morphogenesis at low doses (1 to 20 μM) (Fig. 1). EDG-1 is known to activate the mitogen-activated protein (MAP) kinase known as extracellular signal-regulated kinase 2 (ERK-2) through pertussis toxin (PTx)–sensitive G_i protein (*12*). However, PD98059 and PTx, which inhibit the ERK-2 signaling pathway and trimeric G_i proteins (*13*), respectively, did not inhibit EDG-1–mediated morphogenesis (*8*). However, C3 exotoxin, an inhibitor of Rho (*14*), completely prevented this morphogenesis, suggesting a requirement for Rho (Fig. 1).

HEK293*EDG-1* cells aggregated strongly in suspension, whereas HEK293*pCDNA* cells did not (Fig. 2A). This aggregation was Ca^{2+}-dependent and was completely prevented by EGTA. Incubation with the integrin antagonist RGD peptide did not affect cell-cell aggregation, indicating the lack of involvement of integrins. Cytochalasin B, an inhibitor of microfilaments and nonspecific aggregation of cells, also did not affect cell-cell aggregation. Because the cadherins mediate calcium-dependent homotypic adhesion mechanisms (*15*), we analyzed the amounts of cadherin family polypeptides in HEK293*EDG-1* and HEK293*pCDNA* cells. Expression of both P- and E-cadherins was increased in HEK293*EDG-1* cells (Fig. 2B). However, expression of cytoplasmic cadherin-associated proteins, such as α-, β-, and γ-catenin (*15*), was not altered. Moreover, the expression of focal adhesion kinase and paxillin, which are involved in the formation of focal adhesion complexes (*2*), was also unaltered. The expression of vascular endothelial cadherin (VE-cadherin or cadherin-5) was not observed in either vector- or *EDG*-1–transfected HEK293 cells (*8*). HEK293*EDG-1* cells had abundant well-developed adherens junction–like structures (Fig. 2C). Moreover, consistent with the morphogenetic differentiation, expression of P-cadherin in HEK293*EDG-1* cells was enhanced by FBS and SPP and was blocked in both cases by C3 exotoxin. However, inhibition of the G_i pathway with PTx did not inhibit the EDG-1–induced P-cadherin expression (Fig. 2D). Together, these data suggest that SPP signals through EDG-1 to regulate the biogenesis or the maintenance of the adherens junctional complexes and morphogenetic differentiation. Rho was required for both EDG-1–induced cadherin expression and formation of adherens junctions, consistent with the observation that the small guanosine triphosphatases (GTPases) Rho and Rac are required for the establishment of cadherin-dependent cell-cell contacts (*4*).

To provide further evidence that SPP is a ligand for EDG-1, we developed a radioligand binding assay. Specific ^{32}P-labeled SPP binding was time-dependent and was observed only in HEK293*EDG-1* cells, whereas binding was negligible to vector-transfected cells (Fig. 3A). SPP binding to HEK293*EDG-1* was saturable, and Scatchard analysis indicated a dissociation constant (K_d) of 8.1 nM and a maximum binding capacity of 661 fmol per 10^5 cells (Fig. 3B). Specific binding of [^{32}P]SPP experi-

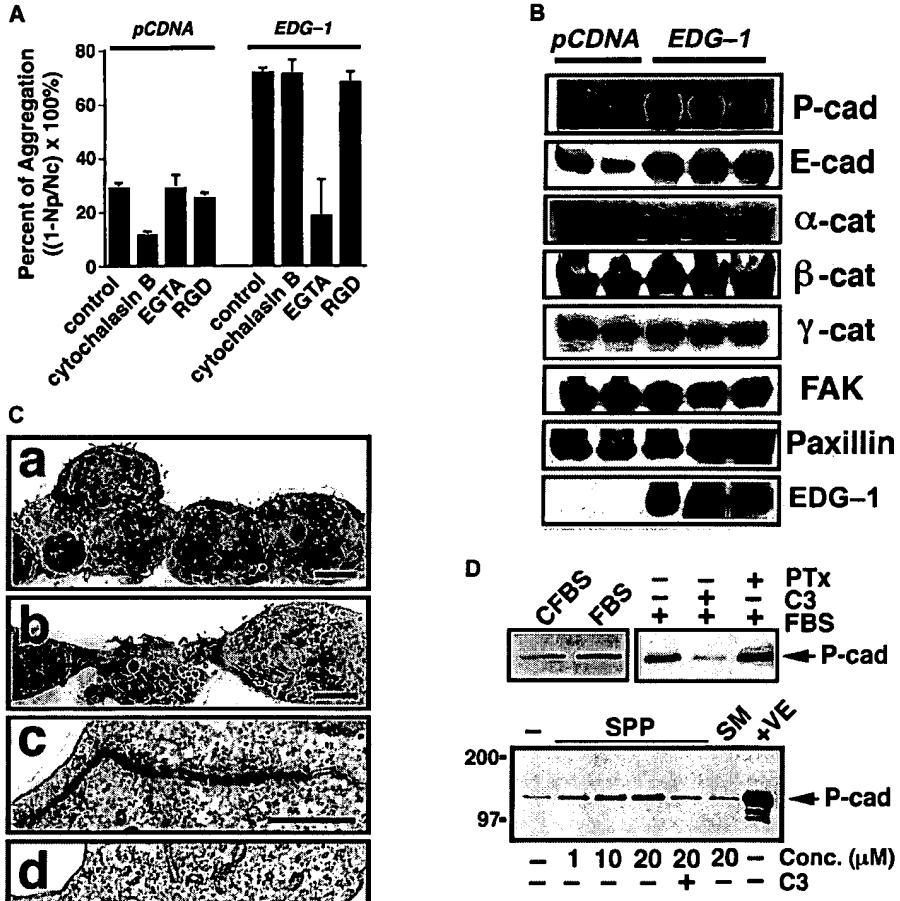

Fig. 2. Mechanisms underlying EDG-1–dependent morphogenesis. (**A**) Induction of calcium-dependent cell-cell aggregation of HEK293*pCDNA* and HEK293*EDG-1* cells was analyzed by the aggregation assay as described (*25*). Cytochalasin B (2 μM), EGTA (5 mM), or RGD peptide (1 mg/ml) was added to the medium before the initiation of the assay. Data represent mean ± SD of triplicate determinations from a typical experiment that was repeated two times. (**B**) Expression of P- and E-cadherin polypeptides. Cell extracts from two HEK293*pCDNA* and three HEK293*EDG-1* independently isolated clones were immunoblotted with various antibodies (Transduction Laboratories, Lexington, Kentucky) or with anti-M2; cad, cadherin; cat, catenin; FAK, focal adhesion kinase. (**C**) Formation of adherens junctions. Transmission electron micrographs of thin sections of HEK293*EDG-1* (a and c) and HEK293*pCDNA* (b and d) cells cultured in the presence of FBS. (a and b) Note the aggregated, clustered nature of HEK293*EDG-1* cells. Scale bar, 5 μm. (c and d) Detail of a representative cell-cell junction from both cell types. Scale bar, 0.5 μm. (**D**) Ligand- and Rho-dependent expression of P-cadherin. HEK293*EDG-1* cells were cultured in FBS (10%), CFBS (10%), or FBS (10%) containing C3 exotoxin (10 μg/ml) or PTx (100 ng/ml) for 3 days (top) or were treated with the indicated concentrations (Conc.) of lipids with or without the C3 exotoxin for 3 days in medium containing CFBS (10%) (bottom). Cell extracts were analyzed for P-cadherin expression by immunoblot analysis. Data are from a representative experiment that was repeated at least two times. SM, sphingomyelin; +VE, positive control P-cadherin protein from A431 cell extracts. The numbers to the left are molecular weight markers.

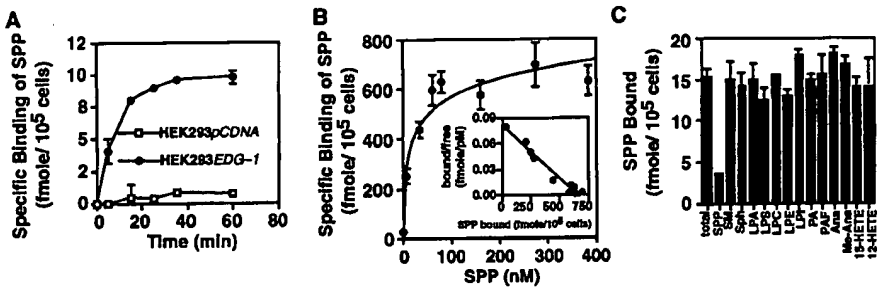

Fig. 3. Binding of SPP to EDG-1 (*26*). (**A**) Time dependence of specific [^{32}P]SPP binding. Cells were incubated with 1 nM [^{32}P]SPP for the indicated times, and specific binding was determined (*26*). (**B**) Binding isotherm of [^{32}P]SPP to HEK293*EDG-1* cells. Cells were incubated with the indicated concentrations of [^{32}P]SPP, and specific binding was measured. The inset shows the Scatchard plot of [^{32}P]SPP binding to HEK293*EDG-1* cells. (**C**) Competition of SPP binding by related lipids. HEK293*EDG-1* cells were incubated in the presence of 1 nM [^{32}P]SPP without or with 100 nM of the indicated lipids, and total binding was measured. Data are means ± SD from a typical experiment, which was repeated at least two times. Sph, sphingosine; LPS, lysophosphatidyl serine; LPC, lysophosphatidyl choline; LPE, lysophosphatidyl ethanol; LPI, lysophosphatidyl inositol; PA, phosphatidic acid; PAF, platelet-activating factor; Ana, anandamide; Me-Ana, methyl anandamide.

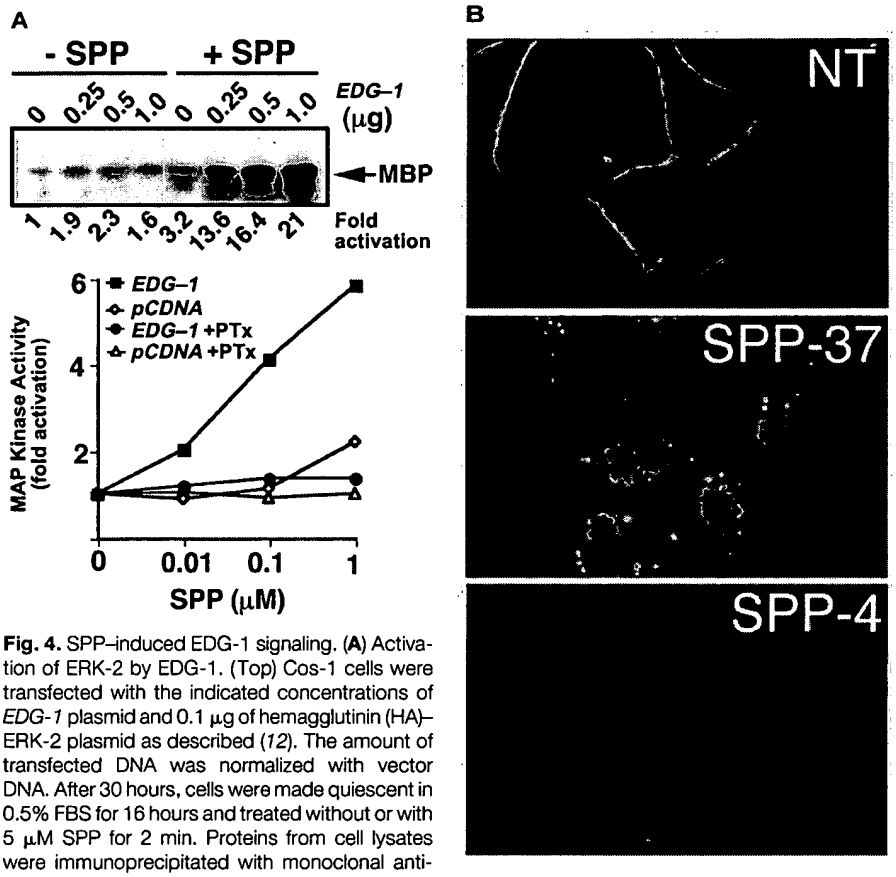

Fig. 4. SPP–induced EDG-1 signaling. (**A**) Activation of ERK-2 by EDG-1. (Top) Cos-1 cells were transfected with the indicated concentrations of *EDG-1* plasmid and 0.1 μg of hemagglutinin (HA)–ERK-2 plasmid as described (*12*). The amount of transfected DNA was normalized with vector DNA. After 30 hours, cells were made quiescent in 0.5% FBS for 16 hours and treated without or with 5 μM SPP for 2 min. Proteins from cell lysates were immunoprecipitated with monoclonal antibody to HA, and ERK-2 kinase activity against the myelin basic protein (MBP) substrate was assayed (*12*). Equal expression of transfected HA–ERK-2 was confirmed by immunoblot analysis with monoclonal antibody to HA. Expression of the FLAG-tagged EDG-1 was confirmed by immunoblot analysis with anti-M2. (Bottom) Cos-1 cells were cotransfected with HA–ERK-2 and 0.25 μg of either *EDG-1* expression vector or vector alone, deprived of serum for 16 hours in the presence or absence of PTx (200 ng/ml), and then stimulated with the indicated concentrations of SPP for 2 min, and ERK-2 activity was measured. Data are expressed as fold activation derived from densitometric scans of autoradiographs. (**B**) Internalization of EDG-1 induced by SPP. HEK293 cells stably transfected with the *EDG-1*–GFP construct (*27*) were incubated for 24 hours in CFBS and treated with 100 nM SPP, and the subcellular localization of EDG-1 was visualized with a Zeiss TV100 fluorescence microscope with a 63× oil immersion lens. SPP-37, cells were treated with SPP for 2 hours at 37°C; SPP-4, cells were treated with SPP for 2 hours at 4°C; NT, no treatment.

enced competition only from unlabeled SPP and not from other lipids that did not induce morphogenetic differentiation (Fig. 3C). Thus, binding of SPP to EDG-1 is of high affinity and high specificity, consistent with the possibility that SPP is a physiological ligand for EDG-1. SPP is present in serum (*16*), where it occurs at concentrations greater than the measured K_d for EDG-1. LPA, another serum-borne lysolipid, signals through the related EDG-2/vzg-1 receptor to regulate cell rounding and serum response factor–dependent transcription (*7*, *17*).

If SPP is a physiological ligand for EDG-1, it should activate EDG-1–regulated signaling pathways. Transfection of cells with *EDG-1* causes G_i-dependent activation of ERK-2 (*12*), and SPP activates ERK-1 and ERK-2 in various cells (*18*). Stimulation of ERK-2 activity by nanomolar concentrations of SPP was potentiated by expression of EDG-1, and this effect was blocked in cells treated with PTx (Fig. 4A). Thus, activation of EDG-1 by SPP transduces two distinct intracellular signaling pathways. First, the G_i protein–coupled ERK-2 pathway is activated. Previous studies have indicated that the βγ subunit of the heterotrimeric G protein activates the small GTPase Ras, which in turn stimulates the ERK pathway (*19*). Second, Rho-coupled pathways that regulate morphogenesis are activated. Activation of the Rho pathway by GPRs is mediated by the G_{12}/G_{13} family of heterotrimeric G proteins (*20*); however, the intermediate signaling steps are poorly understood. Indeed, similar activation of both pathways has been shown for LPA, a related bioactive lipid (*3*, *4*).

Ligand binding to GPRs induces internalization of receptors (*21*). To examine the cellular localization of EDG-1, we expressed the EDG-1 receptor fused with a COOH-terminal green fluorescent protein (GFP). The EDG-1–GFP polypeptide was localized primarily on the plasma membrane (Fig. 4B). Treatment of cells with 100 nM SPP for 2 hours at 37°C caused translocation of EDG-1 into intracellular vesicles. Neither incubation with SPP at 4°C nor incubation with other lipids that do not compete for high-affinity SPP binding to EDG-1 induced receptor trafficking into intracellular vesicles. Moreover, localization of the GFP control polypeptide in the cytosol was not altered by SPP treatment.

SPP, stored in platelets and released by platelet activation, is now recognized as a potent bioactive lipid with multiple biological activities (*22*). Our results reveal a role for SPP as an extracellular ligand for the endothelial-derived receptor EDG-1

that regulates morphogenetic differentiation. Because serum concentrations of SPP are estimated to be 60 times greater than the K_d for binding to EDG-1 (*16*), our data argue that SPP may be a physiologically relevant ligand for EDG-1.

REFERENCES AND NOTES

1. G. M. Edelman, *Annu. Rev. Cell Biol.* **2**, 81 (1986); E. A. Clark, and J. S. Brugge, *Science* **268**, 233 (1995); S. Miyamoto *et al.*, *J. Cell Biol.* **131**, 791 (1995); B. M. Gumbiner, *Cell* **84**, 345 (1996); R. O. Hynes, *ibid.* **69**, 11 (1992).
2. K. Burridge and M. Chrzanowska-Wodnicka, *Annu. Rev. Cell Dev. Biol.* **12**, 463 (1996); R. Montesano, G. Schaller, L. Orci, *Cell* **66**, 697 (1991); C. de Vries *et al.*, *Science* **255**, 989 (1992).
3. W. H. Moolenaar, O. Kranenburg, F. R. Postma, G. C. M. Zondag, *Curr. Opin. Cell Biol.* **9**, 168 (1997); F. Wang, C. D. Nobes, A. Hall, S. Spiegel, *Biochem. J.* **324**, 481 (1997); T. Seufferlein and E. Rozengurt, *J. Biol. Chem.* **270**, 24343 (1995); N. Desai *et al.*, *J. Cell Biol.* **121**, 1385 (1993).
4. V. M. M. Braga, L. M. Machesky, A. Hall, N. A. Hotchin, *J. Cell Biol.* **137**, 1421 (1997); N. Tapon and A. Hall, *Curr. Opin. Cell Biol.* **9**, 86 (1997); K. Takaishi, T. Sasaki, H. Kotani, H. Nishioka, Y. Takai, *J. Cell Biol.* **139**, 1047 (1997); A. Hall, *Science* **279**, 509 (1998).
5. T. Hla and T. Maciag, *J. Biol. Chem.* **265**, 9308 (1990).
6. M. I. Masana, R. C. Brown, H. Pu, M. E. Gurney, M. L. Dubocovich, *Receptors Channels* **3**, 255 (1995); H. Okazaki *et al.*, *Biochem. Biophys. Res. Commun.* **190**, 1104 (1993); F. Yamaguchi, M. Tokuda, O. Hatase, S. Brenner, *ibid.* **227**, 608 (1996).
7. J. H. Hecht, J. A. Weiner, S. R. Post, J. Chun, *J. Cell Biol.* **135**, 1071 (1996).
8. M.-J. Lee and T. Hla, unpublished data.
9. HEK293 fibroblasts were transfected with FLAG epitope–tagged human *EDG-1* cDNA in the *pCDNA-Neo* expression vector as described (*12*). Stably transfected cells were subcloned twice to isolate pure clones. Expression of FLAG-tagged *EDG-1* in transfected clones was verified by immunoblot analysis. Three such clones (HEK293*EDG-1*) and two clones obtained in a similar manner with the vector (HEK293*pCDNA*) were used in the present study.
10. Charcoal-stripped FBS (CFBS) was prepared by incubation of 10 ml of FBS with 1 g of activated charcoal (Sigma) at 4°C overnight. After centrifugation (2000*g* for 10 min), the supernatant was filtered through a 0.22-μm cellulose acetate filter (Corning). Charcoal-bound lipids were eluted with 1 M acetic acid and methanol (1:1). The eluate was vacuum-dried and briefly sonicated in fatty acid–free bovine serum albumin (BSA) (4 mg/ml; Sigma). FBS was extracted three times with 50% (v/v) of butan-1-ol to remove serum-borne lipids.
11. M.-J. Lee and T. Hla, in preparation.
12. M.-J. Lee, M. Evans, T. Hla, *J. Biol. Chem.* **271**, 11272 (1996).
13. L. Pang, T. Sawada, S. J. Decker, A. R. Saltiel, *ibid.* **270**, 13585 (1995); T. Murayama and M. Ui, *ibid.* **258**, 3319 (1983).
14. A. J. Ridley and A. Hall, *Cell* **70**, 389 (1992).
15. M. Takeichi, *Science* **251**, 1451 (1991); ———, S. Hirano, N. Matsuyoshi, T. Fujimori, *Cold Spring Harbor Symp. Quant. Biol.* **57**, 327 (1992); S. Hirano, N. Kimoto, Y. Shimoyama, S. Hirohashi, M. Takeichi, *Cell* **70**, 293 (1992).
16. Y. Yatomi *et al.*, *J. Biochem.* **121**, 969 (1997).
17. S. An, M. A. Dickens, T. Bleu, O. G. Hallmark, E. J. Goetzel, *Biochem. Biophys. Res. Commun.* **231**, 619 (1997).
18. J. Wu, S. Spiegel, T. W. Sturgill, *J. Biol. Chem.* **270**, 11484 (1995); O. Cuvillier *et al.*, *Nature* **381**, 800 (1996); S. Pyne, J. Chapman, L. Steele, N. J. Pyne, *Eur. J. Biochem.* **237**, 819 (1996).
19. W. J. Koch, B. E. Hawes, L. F. Allen, R. J. Lefkowitz, *Proc. Natl. Acad. Sci. U.S.A.* **91**, 12706 (1994); T. van Biesen *et al.*, *Nature* **376**, 781 (1995); P. L. Hordijk, I. Verlaan, E. J. van Corven, W. H. Moolenaar, *J. Biol. Chem.* **269**, 645 (1994).
20. A. M. Buhl, N. L. Johnson, N. Dhanasekaran, G. L. Johnson, *J. Biol. Chem.* **270**, 24631 (1995).
21. S. Mukherjee, R. N. Ghosh, F. R. Maxfield, *Physiol. Rev.* **77**, 759 (1997); S. K. Bohm, E. F. Grady, N. W. Bunnett, *Biochem. J.* **322**, 1 (1997); S. S. G. Ferguson *et al.*, *Science* **271**, 363 (1996).
22. Y. Yatomi, F. Ruan, S. Hakomori, Y. Igarashi, *Blood* **86**, 193 (1995); S. Spiegel and A. H. Merrill Jr., *FASEB J.* **10**, 1388 (1996).
23. H. Takeda *et al.*, *J. Cell Biol.* **131**, 1839 (1995).
24. A. Olivera and S. Spiegel, *Nature* **365**, 557 (1993).
25. Aggregation assays were done essentially as described (*23*), with minor modifications. Single-cell suspensions were plated into dishes coated with 1% agarose and rotated at 80 revolutions per minute for 90 min at 37°C to allow aggregation. Quantitative analysis of cell aggregation was performed with a Coulter (Miami, FL) Particle Counter with an aperture size of 100 μm. The extent of cell aggregation is represented by the index $(1 - N_p/N_c) \times 100\%$, where N_p and N_c are the total number of particles counted and the total number of cells used, respectively.
26. [^{32}P]SPP was synthesized enzymatically with partially purified sphingosine kinase as described previously (*24*). HEK293*pCDNA* or HEK293*EDG-1* cells (10^5) were incubated at 4°C in 200 μl of binding buffer [20 mM tris-HCl (pH 7.4), 100 mM NaCl, 15 mM NaF, 2 mM deoxypyridoxine, 0.2 mM phenylmethylsulfonyl fluoride, aprotinin (1 μg/ml), leupeptin (1 μg/ml), and fatty acid–free BSA (4 mg/ml)], with the indicated concentration of [^{32}P]SPP for 30 min in the absence or presence of unlabeled lipid competitors. Cells were pelleted at low speed in a microcentrifuge and washed twice with binding buffer containing fatty acid–free BSA (0.4 mg/ml). Bound [^{32}P]SPP was quantitated by scintillation counting. Specific binding was calculated as total binding minus binding in the presence of 100-fold excess of unlabeled SPP.
27. The enhanced GFP cDNA (Clontech, Palo Alto, CA) was fused at the COOH-terminus of the *EDG-1* cDNA, and the chimera was cloned into a eukaryotic expression vector containing a cytomegalovirus promoter (*pEGFP*). Expression of the correct polypeptide was confirmed by DNA sequencing as well as by immunoblot analysis of transfected cells. HEK293 clones stably expressing EDG-1–GFP were isolated by standard procedures (*12*).

28. We thank R. D. Berlin and T. Maciag for support and discussions and T. I. Bonner for sharing unpublished results. Supported by research grants from the NIH to T.H. (DK45659 and HL49094) and S.S. (GM43880 and CA61774) and by a grant from the American Cancer Society (BE-275) to S.S.

20 November 1997; accepted 3 February 1998

Identification of the natural ligand of an orphan G-protein-coupled receptor involved in the regulation of vasoconstriction

Hans-Peter Nothacker*, Zhiwei Wang*, Anne Marie McNeill*, Yumiko Saito*, Sven Merten*, Brian O'Dowd†, Sue P. Duckles* and Olivier Civelli*‡§

*Department of Pharmacology, University of California at Irvine, Irvine, California 92697-4625, USA
†Department of Pharmacology and Medicine, University of Toronto, Toronto, Ontario M5S 2S1, Canada
‡Department of Developmental and Cell Biology, University of California at Irvine, Irvine, California 92697-4625, USA
§e-mail: ocivelli@uci.edu

Homology-based cloning approaches and genome-sequencing efforts have revealed the existence of a large number of human genes encoding 'orphan' G-protein-coupled receptors (GPCRs), receptors that bind unidentified natural ligands. Discovery of these natural ligands is the first necessary step in understanding the biological significance of the orphan GPCRs. We[1] and others[2] have developed an approach by which to successfully isolate endogenous ligands from complex tissue libraries. This approach, referred to as the orphan-receptor strategy[3], uses orphan receptors as baits to isolate their native ligand from tissue extracts and has been successfully applied to identify new neuropeptides[4–6]. Here we apply this strategy to the orphan receptor GPR14 and show that it binds the bioactive peptide known as urotensin II.

The complementary DNA encoding the orphan receptor GPR14, or SENR, was cloned using degenerate oligonucleotides directed at conserved regions of known GPCRs[7,8]. Phylogenetic analysis positioned the GPR14 sequence closely to somatostatin, opioid and galanin receptors[8], indicating that the endogenous ligand of GPR14 may also be peptidergic. We set out to identify the natural ligand of GPR14 from peptide extracts prepared from a variety of different mammalian tissues. Extracts were fractionated by preparative reverse-phase high-performance liquid chromatography (rpHPLC) into 72 individual fractions, and aliquots were tested for induction of changes in intracellular Ca^{2+} ($[Ca^{2+}]_i$) in Chinese hamster ovary (CHO) cells transiently transfected with GPR14 cDNA. Intracellular Ca^{2+} changes were monitored using a fluorescence imaging plate reader (FLIPR) system[9]. A reproducible and robust change in Ca^{2+} concentration was observed in two adjacent fractions (Fig. 1a). This change could not be detected either in non-transfected cell lines or in cells transfected with other orphan receptors. Highest levels of activity were detected in bovine hypothalamic tissue, which was consequently used for large-scale purification. The active component was purified over a seven-step purification strategy combining reverse-phase and cationic-exchange HPLCs. One single activity peak was detected, indicating that the activity can be attributed to a unique molecular entity. The bioactive compound was extremely scarce, preventing us from carrying out a total structural analysis. However, the Ca^{2+} response to the active material showed a distinctive time course (Fig. 1a, inset). Furthermore, the active material was sensitive to trypsin (Fig. 1a, inset) and alkylating agents, leading us to conclude that the biological activity could be attributed to a peptide containing basic amino acid(s) and alkylation-sensitive amino acids.

As GPR14 is similar to the somatostatin receptors we decided to screen somatostatin-like, cysteine-bridge-containing peptides on GPR14 and to compare their biological activities and physicochemical properties with that of the endogenous compound identified in our purification scheme. Peptides tested were human melanin-concentrating hormone (MCH), somatostatin-14 (SST-14) and cortistatin-14 and urotensin II. Whereas MCH was inactive, SST-14 and the related peptide cortistatin activated GPR14, albeit only at very high concentrations (Table 1). In contrast, urotensin II induced a robust increase in $[Ca^{2+}]_i$, with a median effective concentration (EC_{50}) of 0.14 nM (Table 1), showing a potency more than 25,000-fold greater than that of SST-14.

Urotensin II was originally isolated from goby[10], and an expressed sequence tag has been described[11] that codes for a human counterpart. We therefore synthesized the mammalian peptide (Table 1) and tested it on GPR14-expressing CHO cells. The time course of the Ca^{2+} response caused by the synthetic peptide was identical to that observed with the active fractions isolated from bovine tissue extracts (Fig. 1a, inset), indicating that the synthetic as well as natural compounds act on the same receptor. The fact that urotensin II activates GPR14 with very high affinity, together with the paucity of urotensin II in the tissue extracts, explains our inability to isolate it in sufficient quantities to allow for structural determination. An active compound from brain extracts of squirrel monkeys eluted on rpHPLC with the same retention time as synthetic human urotensin II peptide (arrow in Fig. 1a), further suggesting that the monitored activity is indeed caused by urotensin II. The activity found in bovine tissue eluted slightly later than human urotensin II, indicating that there may be some structural differences among the mammalian urotensin II peptides.

To develop a urotensin II analogue that would be suitable for binding studies, we synthesized the human urotensin II orthologue

Table 1 Pharmacological profiles of GPR14 and SSTR2A

Peptides	Sequence	Ca^{2+} assay	
		GPR14 (EC_{50} ± s.e.m.; nM)	SSTR2A (EC_{50} ± s.e.m.; nM)
hUII	ETPDCFWKYCV	0.10 ± 0.07	>2,000
[I-Tyr$_9$] hUII		0.35 ± 0.05	ND
[I_2-Tyr$_9$] hUII		2.63 ± 0.30	ND
Urotensin II (goby)	AGTADCFWKYCV	0.14 ± 0.02	ND
[D-Trp$_7$]UII-(5-10)	Ac-CFWKYC-a	19.20 ± 5.76	ND
RC-160	FCYWKVCW-a	338.0 ± 53.6	1.45 ± 0.44
Octreotide	FCFWKTCT-ol	4,270 ±460	1.38 ± 0.39
Somatostatin-14	AGCKNFFWKTFTSC	3,670 ± 460	0.80 ± 0.19
Cortistatin-14	PCKNFFWKTFSSCK	>10,000	ND

ND, not determined. Cysteine residues form intramolecular disulphide bonds. 'a' indicates an C-terminal amide. Ac, acetyl; -ol, reduction of the carboxyl group to an alcohol. Underlined letters indicate D-amino-acid residues. Values represent the means ± s.e.m. of three independent experiments done in triplicate.

(hUII) and iodinated it (Table 1). Monoiodo-hUII induced a concentration-dependent transient increase in Ca^{2+} concentration in stably transfected CHO cells with an EC_{50} similar to that of the unmodified peptide (Table 1), whereas the diiodo form of hUII showed a 25-fold decrease in potency compared with urotensin II. We therefore used the monoiodinated form of hUII as a radioligand for the determination of physical constants. ^{125}I-labelled hUII exhibited saturable and displaceable binding to membranes of cells transfected with GPR14, with an apparent dissociation constant (K_d) of 70 pM and a maximal binding capacity (B_{max}) of 350 fmol per milligram of membrane protein (Fig. 1b).

To define the pharmacological profile of GPR14, we tested peptides structurally related to urotensin II for their ability to activate GPR14-expressing cells. Goby urotensin II, which is identical to hUII at the carboxy terminus but differs in its amino terminus, was equipotent to hUII (Table 1), pointing to the cyclic ring structure as an important binding motif. On the basis of molecular modelling data, a putative urotensin II antagonist, [D-Trp$_7$]UII-(5-10), has been proposed[12] (Table 1). In our assay system, [D-Trp$_7$]UII-(5-10) behaved as an agonist with a 190-fold lower potency compared with the natural urotensin II, but no antagonistic activity at concentrations up to 1 μM could be detected. Because of the structural similarities between the somatostatin and urotensin systems, we tested the somatostatin analogues RC-160 and octreotide (Table 1) for

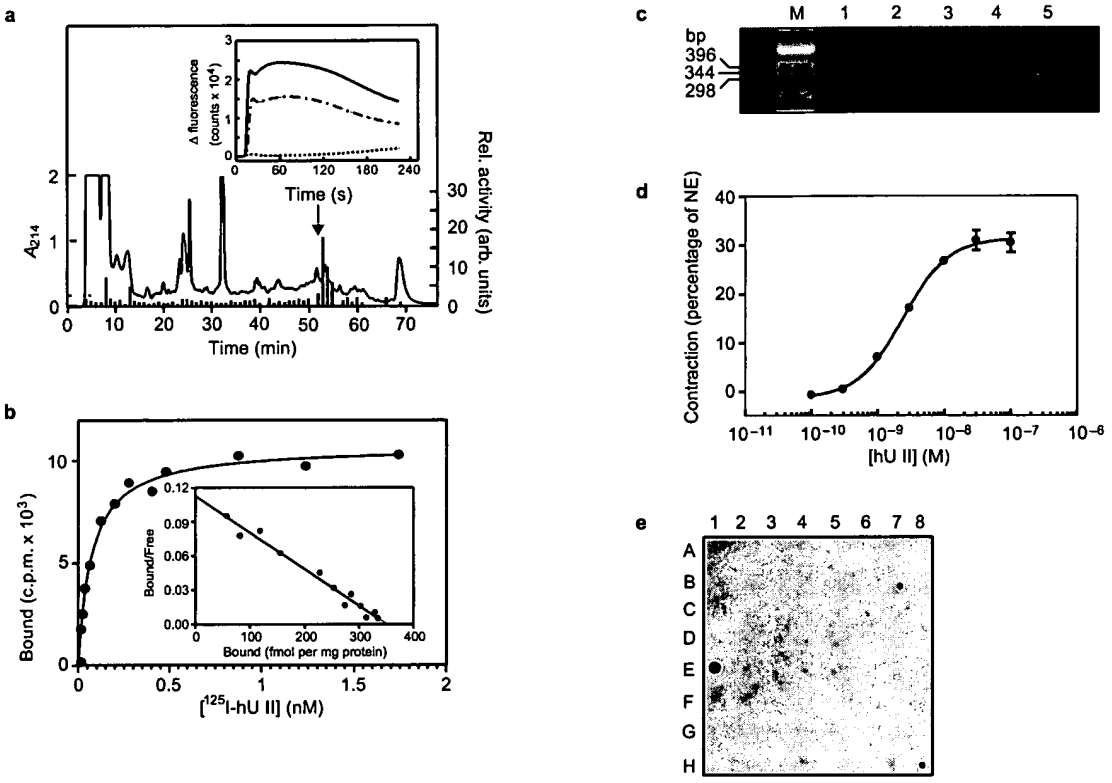

Figure 1 Identification of urotensin II as the endogenous ligand of GPR14. **a**, rpHPLC profile of a bovine hypothalamic tissue extract and corresponding activity of 72 1-min fractions tested for Ca^{2+} mobilization in GPR14-expressing CHO cells. The tissue was treated as described in Methods, and 2.5% of each fraction was tested for the ability to mobilize Ca^{2+} in CHO cells transiently transfected with a GPR14 plasmid[7] and loaded with the calcium-sensitive dye fluo-3. Changes in fluorescence were monitored over 240 s using a FLIPR[9]. The maximal fluorescence increment generated by each fraction on GPR14-transfected cells was normalized to the maximal control value seen in mock-transfected cells. Fractions 53 and 54 were most active. The arrow indicates the elution time of synthetic hUII. The inset shows a comparison of Ca^{2+} kinetics induced by hUII and fraction 53. hUII (0.1 nM, solid line) or 2.5% of fraction 53 (dotted/dashed line) was applied to GPR14-expressing CHO cells, and fluorescence changes were monitored as described above. Treatment of fraction 53 with trypsin (dotted line) abolished the activity of this fraction. **b**, Saturation binding of ^{125}I-labelled hUII to GPR14. Membranes of CHO cells stably expressing GPR14 were incubated with the indicated concentrations of ^{125}I-labelled hUII. Bound ligand was separated by filtration. Concentrations of free ligand were calculated by subtracting the amount of specifically bound ligand from the total amount of radioligand added. The data represent the average of two independent experiments done in triplicate. The insert shows a Scatchard transformation of the specific binding data. **c**, Expression profile of GPR14 in rat cardiovascular tissue as assessed by qualitative reverse transcription with PCR analysis. PCR was done as described in Methods and the reaction products separated on a 1% agarose gel. M, molecular-mass marker; 1, negative control; 2, thoracic aorta; 3, abdominal aorta; 4, heart; 5, positive-control plasmid, bp, base pairs. **d**, Contraction of thoracic aorta strips induced by increasing concentrations of hUII. Contraction induced by hUII is expressed as the percentage of the maximum change in tension induced by norepinephrine (NE). Bars indicate the s.e.m. of four independent experiments. **e**, Tissue distribution of human preprourotensin II (pphUII). Human masterblot (Clontech) was probed with a full length pphUII cDNA (IMAGE number 926809) as recommended by the manufacturer. The tissues are: A1, whole brain; A2, amygdala; A3, caudate nucleus; A4, cerebellum; A5, cerebral cortex; A6, frontal lobe; A7, hippocampus; A8, medulla oblongata; B1, occipital lobe; B2, putamen; B3, substantia nigra; B4, temporal lobe; B5, temporal lobe; B6, subthalamic nucleus; B7, spinal cord; C1, heart; C2, aorta; C3, skeletal muscle; C4, colon; C5, bladder; C6, uterus; C7, prostate; C8, stomach; D1, testis; D2, ovary; D3, pancreas, D4, pituitary; D5, adrenal; D6, thyroid; D7, salivary; D8, mammary gland; E1, kidney; E2, liver; E3, small intestine; E4, spleen; E5, thymus; E6, peripheral leukocytes; E7, lymph nodes; E8, bone marrow; F1, appendix; F2, lung; F3, trachea; F4, placenta; G1, fetal brain; G2, fetal heart; G3, fetal kidney; G4, fetal liver; G5, fetal spleen; G6, fetal thymus; G7, fetal lung; H1, yeast total RNA; H2, yeast transfer RNA; H3, *E. coli* tRNA; H4, *E. coli* DNA; H5, poly(A)$^+$ ribosomal RNA; H6, human C_0t1 DNA; H7, human DNA (100ng); H8, human DNA (500 ng).

their ability to activate GPR14. RC-160 activated the receptor with an EC_{50} of 338 ± 53.6 nM. Octreotide showed even lower potency. SST-14 itself proved to be active on GPR14-expressing cells but at physiologically non-relevant concentrations (Table 1). Cortistatin-14, which differs from SST-14 in a C-terminal lysine residue, exhibited even lower affinity, indicating the importance of having an uncharged C terminus for GPR14 reactivity. On the other hand, hUII was unable to activate the somatostatin 2A receptor (SSTR2A), whereas RC-160 and octreotide mobilized $[Ca^{2+}]_i$ in these cells with a high affinity similar to published values[13]. We thus conclude that urotensin II is the only endogenous high-affinity ligand for the somatostatin-like GPR14 to be detected in our peptidic brain extracts. Activation of GPR14 stimulated Ca^{2+} influx, suggesting a possible physiological role as an excitatory receptor, in contrast to somatostatin receptors which are coupled to inhibition of adenylate cyclase.

GPR14 has been reported to be expressed in heart, retina, cerebellum and choroid plexus[8]. Furthermore, urotensin II has been shown to have physiological actions in the mammalian cardiovascular system[14], and specific binding sites for fish urotensin II on rat thoracic aortic membranes have been reported[15]. We therefore tested whether GPR14 messenger RNA is expressed in the cardiovascular system and found that GPR14 is expressed in rat heart, pulmonary artery and thoracic aorta (Fig. 1c). The presence of GPR14 in thoracic aorta led us to test whether hUII is able to cause contractions of vascular smooth muscle. hUII acted as a vasoconstrictor in a concentration-dependent manner, with an EC_{50} of 2.4 nM (Fig. 1d). Maximal activity reached 32% of norepinephrine-induced contraction. The response was characterized by a delayed onset (10–15 min) and a long-lasting tone, which could not be washed out even after 1 h of frequent changes of the bath solution. Contraction of aortic smooth muscle cells by fish urotensin II has been shown to be Ca^{2+} dependent and to be blocked by the Ca^{2+}-channel-blocker nitrendipine[16]. As shown above, GPR14 activation induces a strong Ca^{2+} influx in CHO cells (Fig. 1a, inset), showing that GPR14 has the pharmacological profile of the receptor responsible for hUII-directed contraction of rat thoracic aorta.

The next question related to the source of cardiovascular urotensin II. Using a normalized northern dot blot of 50 different human tissue samples, we found that human preprourotensin (pphUII) mRNA was expressed at high levels only in human kidney (Fig. 1e). Moderate to low expression was found in spinal cord and medulla oblongata, respectively, but these are not expected to be a source of circulating urotensin II. All other tissues studied expressed either none or very low amounts of precursor. Our data showing high expression of pphUII mRNA in kidney differ from previous results[11], which showed a moderate expression of pphUII mRNA in this organ. The reason for this discrepancy is unknown but may indicate that pphUII mRNA is highly regulated among different individuals.

We conclude that we have identified GPR14 as a receptor for mammalian urotensin II. The expression of GPR14 in rat thoracic aorta correlates with the physiological action of hUII in this tissue. High expression of pphUII in human kidney indicates that the kidney may be the peripheral source of urotensin II that modulates vascular function. Our findings should aid in understanding the role of urotensin II in the mammalian cardiovascular system by allowing the development of agonists and antagonists for the urotensin II receptor. □

Methods

Tissue extraction and partial purification.

Bovine tissues obtained from the local slaughterhouse were minced and immediately boiled for 10 min in deionized water at a 1:2 tissue:water (g:ml) ratio. After cooling to 10°C, acetic acid was added to a final concentration of 1 M. The homogenate was further treated with a Polytron for 2 min. After centrifugation for 30 min at 12,000*g*, the supernatant was removed and the pellet re-extracted with one volume of 1 M acetic acid. The supernatants were combined, and three volumes acetone were added. The precipitate was removed at 15,000*g* for 30 min. After concentration of the supernatant by rotor evaporation the remainder was extracted two times with two volumes of ethylether, then frozen and lyophilized. The lyophilized material was resuspended in 5% CH_3CN and 0.1% trifluoroacetic acid (TFA) and applied on a PrepPak-Delta-Pak C18, 15 μm, 300 A, 25 × 100 mm (Waters), pre-equilibrated with 5% CH3CN/ 0.1% TFA. The material was eluted with a linear gradient from 5% to 39% CH_3CN/0.1% TFA. The active fractions eluting at 34–38% CH_3CN were collected.

Radioligand-binding assay.

hUII was iodinated according to the method of ref. 17 using iodo-beads (Pierce). Initially, synthetic hUII (3 nmol) was iodinated with 15 nmol NaI in 50 mM phosphate buffer, pH 7.4, and incubated for 10 min at room temperature. The reaction mixture was immediately loaded on a Waters Nova-Pak C18 3.9 × 150 mm analytical column equilibrated with 16% CH3CN/0.1% TFA at a flow rate of 1 ml min^{-1}. Reaction products were eluted with a linear gradient to 60% CH_3CN/0.1% TFA over 35 min. Peaks were monitored at 215 nm, manually collected and tested for identity by matrix-assisted laser desorption mass spectrometry. [^{125}I-Tyr_9]hUII was synthesized as described above using 0.5 nmol hUII and 500 μCi $Na^{125}I$ (Amersham). Ligand-binding assays were done in 96-well glass fibre type-B filtration plates (Millipore) precoated with 0.5% BSA at room temperature for 1 h. CHO cells stably expressing GPR14 were collected and resuspended in binding buffer (20 mM Tris-HCl, pH 7.4, 2 mM $MgCl_2$, 0.25% BSA and 0.25 mg ml^{-1} bacitracin). Membranes were prepared using a Polytron tissue homogenizer. Total membrane particulate was obtained after centrifugation at 20,000*g* for 60 min at 4°C. The resulting pellet was passed through a 27-gauge needle five times and membranes were stored at −80°C until use. Protein concentration was determined using a BCA protein assay kit (Pierce). Membranes (5 μg total protein) were incubated with monoiodinated [^{125}I-Tyr_9]hUII for 60 min in a total volume of 200 μl binding buffer. Filters were washed with cold PBS three times and radioactivity was counted using a MicroBeta liquid scintillation counter (EG&G Wallac, Gaithersburg, MD). Nonspecific binding was determined in the presence of 1 μM unlabelled hUII. Data were analysed using PRISM software (GraphPad, San Diego, CA).

GPR14-expression analysis.

Reverse-transcription reactions were done with Superscript II reverse transcriptase (Life Technologies) using 5 μg total tissue RNA. 10% of the final reaction products were used in polymerase chain reactions (PCRs) containing 0.2 μM each of primers 5′-CTGAGCCTGGAGTCTACAACAAGC and 5′-TAGGTGGCTATGATGAAGGGAATG, respectively. Reactions were carried out using Goldtaq polymerase (Perkin Elmer) and buffer conditions as recommended by the manufacturer. PCR conditions: 94°C for 10 min followed by 34 cycles of 94°C for 30 s, 58°C for 30 s and 72°C for 60 s. For negative controls, template cDNA was replaced by water.

Thoracic aorta contraction assay.

4-month-old male Fischer 344 rats were killed by decapitation and their thoracic aorta removed. Arteries were cut into 3-mm segments and mounted on platinum wires in a oxygenated tissue bath containing 40 ml Krebs solution (in mM: 118 NaCl, 5.2 KCl, 1.6 $CaCl_2$, 1.2 KH_2PO_4, 25.5 $NaHCO_3$, 1.2 $MgSO_4$, 0.027 disodium EDTA, and 115 glucose) kept at 37°C and oxygenated with 95% O_2/5% CO_2. Tissue segments were slowly stretched to 1 g resting tension, then allowed to equilibrate for 1 h, with fresh Krebs solution added every 20 min. Contractile responses to cumulative addition of hUII (10^{-10}–10^{-7} M) were recorded using Fort 10 force transducers and a MacLab analog-to-digital converter. Maximal contraction of each arterial segment was then determined by addition of 10^{-4} M norepinephrine, and endothelial integrity confirmed by measuring relaxation to acetylcholine (10^{-4} M).

RECEIVED 5 AUGUST 1999; REVISED 18 AUGUST 1999; ACCEPTED 18 AUGUST 1999; PUBLISHED 16 SEPTEMBER 1999.

1. Reinscheid, R. K. *et al. Science* 270, 792–794 (1995).
2. Meunier, J. C. *et al. Nature* 377, 532–535 (1995).
3. Civelli, O. *FEBS Lett.* 430, 55–58 (1998).
4. Sakurai, T. *et al. Cell* 92, 573–585 (1998).
5. Tatemoto, K. *et al. Biochem. Biophys. Res. Commun.* 251, 471–476 (1998).
6. Hinuma, S. Y. *et al. Nature* 393, 272–276 (1998).
7. Marchese, A. *et al. Genomics* 29, 335–344 (1995).
8. Tal, M. *et al. Biochem. Biophys. Res. Commun.* 209, 752–759 (1995).
9. Coward, P. *et al. Proc. Natl Acad. Sci. USA* 95, 352–357 (1998).
10. Pearson, D. *et al. Proc. Natl Acad. Sci. USA* 77, 5021–5024 (1980).
11. Coulouarn, Y. *et al. Proc. Natl Acad. Sci. USA* 95, 15803–15808 (1998).
12. Perkins, T. D., Bansal, S. & Barlow, D. J. *Biochem. Soc. Trans.* 18, 918–919 (1990).
13. Patel, Y. *et al. Life Sci.* 57, 1249–1265 (1995).
14. Gibson, A., Wallace, P. & Bern, H. A. *Gen. Comp. Endocrinol.* 64, 435–439 (1986).
15. Gibson, A., Conyers, S. & Bern, H. A. *J. Pharm. Pharmacol.* 40, 893–895 (1988).
16. Itoh, H., McMaster, D. & Lederis, K. *Eur. J. Pharmacol.* 149, 61–66 (1988).
17. Markwell, M. A. *Anal. Biochem.* 125, 427–432 (1982).

ACKNOWLEDGEMENTS

This work was supported by a grant from the NIH and by the endowment of the Eric and Lila Nelson Chair in Neuropharmacology. We thank D. Knauer for help with iodinations, R. Reinscheid for editorial assistance and S. Lin for helpful discussions.

Correspondence and requests for materials should be addressed to O.C.

Apoptosis Mediated by Activation of the G Protein-Coupled Receptor for Parathyroid Hormone (PTH)/ PTH-Related Protein (PTHrP)

Paul R. Turner, Suzanne Mefford, Sylvia Christakos, and Robert A. Nissenson

Endocrine Unit (P.R.T., S.M., R.A.N.)
Veterans Affairs Medical Center and the Departments of Medicine and Physiology
University of California San Francisco
San Francisco, California 94121

Department of Molecular Biology and Biochemistry (S.C.)
New Jersey Medical School
Newark New Jersey 07103

The present studies were carried out to evaluate the mechanisms by which PTH/PTHrP receptor (PTHR) activation influences cell viability. In 293 cells expressing recombinant PTHRs, PTH treatment markedly reduced the number of viable cells. This effect was associated with a marked apoptotic response including DNA fragmentation and the appearance of apoptotic nuclei. Similar effects were evidenced in response to serum withdrawal or to the addition of tumor necrosis factor (TNFα). Addition of caspase inhibitors or overexpression of bcl-2 partially abrogated apoptosis induced by serum withdrawal. Caspase inhibitors also protected cells from PTH-induced apoptosis, but overexpression of bcl-2 did not. The effects of PTH on cell number and apoptosis were neither mimicked by activators of the cAMP pathway (forskolin, isoproterenol) nor blocked by an inhibitor (H-89). However, elevation of Ca_i^{2+} by addition of thapsigargin induced rapid apoptosis, and suppression of Ca_i^{2+} by overexpression of the calcium- binding protein, calbindin D28k, inhibited PTH-induced apoptosis. The protein kinase C inhibitor GF 109203X partially inhibited PTH-induced apoptosis. Regulator of G protein signaling 4 (RGS4) (an inhibitor of the activity of the α-subunit of G_q) suppressed apoptotic signaling by the PTHR, whereas the C-terminal fragment of GRK2 (an inhibitor of the activity of the $\beta\gamma$-subunits of G proteins) was without effect. Chemical mutagenesis allowed selection of a series of 293 cell lines resistant to the apoptotic actions of PTH; a subset of these were also resistant to TNFα. These results suggest that 1) apoptosis produced by PTHR and TNF receptor signaling involve converging pathways; and 2) Gq-mediated phospholipase C/Ca^{2+} signaling, rather than Gs-mediated cAMP signaling, is required for the apoptotic effects of PTHR activation. (Molecular Endocrinology 14: 241–254, 2000)

0888-8809/00/$3.00/0
Molecular Endocrinology

INTRODUCTION

Apoptosis or programmed cell death is a process fundamental to normal growth and development, immune response, and tissue remodeling after injury or insult. The mammalian signal transduction pathways that mediate apoptosis, although under intense scrutiny, remain incompletely understood. Recently, it has become apparent that apoptosis is a crucial process in skeletal development and homeostasis and that signaling by the PTH /PTH-related protein (PTHrP) receptor (PTHR) can either promote or suppress apoptosis depending on the cellular context (1, 2). In addition, growth- suppressive effects of PTHR activation have been reported in osteoblastic target cells (3–5). The PTHR is known to be capable of signaling in response to PTH or PTHrP via two G protein-coupled pathways: 1) Gq-mediated activation of phospholipase C (PLC), resulting in increased Ca_i^{2+} and activation of protein kinase C (PKC); and 2) Gs-mediated activation of adenylyl cyclase leading to cAMP production and protein kinase A (PKA) activation (6). However, it is unclear whether either or both of these signaling pathways are linked to changes in PTH-induced cell proliferation or apoptosis.

Embryonic mice lacking expression of functional PTHrP or PTHR gene products display severe abnormalities of endochondral bone formation (7, 8). The

acceleration of chondrocyte differentiation and disorganization of the growth plate seen in these mice underscores the important role that PTHR signaling and apoptosis play in normal skeletal growth and differentiation (1, 9). In addition, the skeletal abnormalities that are observed in Jansen's metaphyseal chondrodysplasia have been attributed to point mutations in the PTHR, which result in constitutively active mutant PTHRs (10, 11). The mechanisms by which PTHrP and PTHR signaling affect skeletal development are not known, although feedback between PTHR signaling and Indian hedgehog has been proposed to modulate chondrocyte differentiation (12).

Terminal differentiation of chondrocytes is associated with apoptosis (13), and PTHrP has been shown to increase expression of the antiapoptotic gene bcl-2 coincident with suppressing terminal chondrocyte differentiation (1). However, preliminary studies indicate that PTH administration to young rats promotes the apoptosis of osteoblasts and osteocytes *in vivo* (2). This suggests that apoptosis can be initiated by activation of the PTHR, and that this is likely to contribute to the spectrum of physiological responses to PTH and/or PTHrP. In the present study, we report that PTH induces apoptosis in human embryonic kidney (HEK) 293 cells stably expressing the PTHR. These effects require the second messenger products of PLC signaling, but are independent of adenylyl cyclase signaling.

RESULTS

Initial studies were carried out to determine the effects of PTHR signaling on cell viability. The wild-type (Wt) opossum PTHR was stably expressed in 293 cells, which lack endogenous PTHRs. Exposure of these cells to a PTHR agonist, bovine (b) PTH(1–34), resulted in a time- and dose-dependent decrease in cell number (Fig. 1). As little as 1 nM bovine (b)PTH(1–34) produced a significant effect, and 1 μM bPTH(1–34) reduced the number of cells by approximately 80% within 48–72 h. Serum withdrawal, known to induce apoptosis in 293 cells (14), resulted in decreased cell numbers after 72 h. Addition of bPTH(1–34) had no effect on the number of control 293 cells (transfected with vector alone), and addition of a PTHR antagonist [bPTH(7–34), 1 μM], did not alter the number of PTHR-expressing 293 cells (not shown).

To determine whether inhibition of cell number by PTH was associated with apoptosis, we obtained a quantitative index of the amount of DNA fragmentation in response to either PTH treatment or serum withdrawal. Cells were fixed at various time points after commencement of PTH treatment or serum withdrawal, and terminal deoxynucleotidyl transferase-mediated dUTP nick end labeling (TUNEL) assays were used to label terminal DNA fragments. Positive staining was readily detected in apoptotic cells (Fig. 2A). Analysis of TUNEL assay results revealed that both serum withdrawal and PTH treatment induced apoptosis in more than 20% of cells after 72 h (Fig. 2B). Similar results were obtained in two additional clonal cell lines of 293 cells expressing the PTHR (not shown). The percent of cells with apoptotic nuclei after serum withdrawal (33%) was similar to that previously reported for serum-deprived 293 cells (14). DNA fragmentation was also visualized using agarose gel electrophoresis of DNA extracts from cells after exposure to PTH or after serum withdrawal (Fig. 2C). The classical DNA ladder of 128-bp DNA fragments was not visible among a more general smear of degraded DNA after treatment with bPTH(1–34), the phorbol ester PMA, or serum withdrawal. The PTHR antagonist [PTH(7–34), 1 μM], did not induce visible DNA degradation. Very little DNA fragmentation was observed in control cells by either TUNEL staining or gel electrophoresis. These results show that apoptosis occurs only infrequently in proliferating 293 cells. PTH did not elicit an apoptotic response in 293 cells in the absence of PTHR expression (not shown).

Differences in cell morphology after PTH treatment and serum withdrawal were observed. The morphological response to serum withdrawal was cell shrinkage/cell rounding (Fig. 3A), a response frequently associated with apoptosis (15). The initial morphological response to PTH treatment was cell spreading and flattening (Fig. 3A). Fluorescent labeling of the actin cytoskeleton with rhodamine-conjugated phalloidin demonstrated major cytoskeletal reorganization after PTHR activation (not shown). The relationship be-

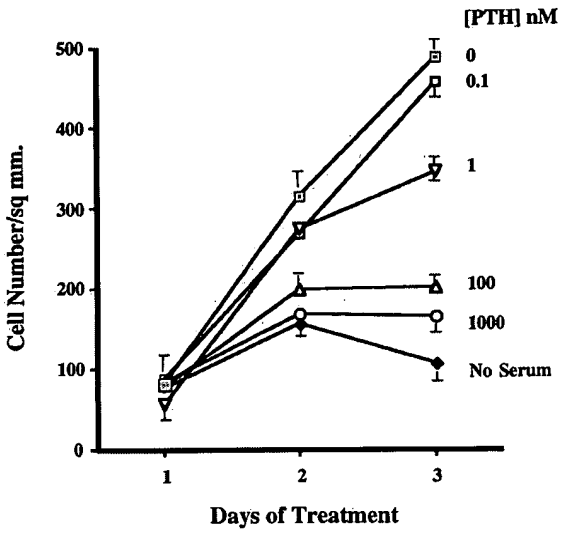

Fig. 1. Effect of bPTH(1–34) on the Number of HEK 293 Cells Expressing the Wt PTHR

Cells were plated at approximately 50 cells/mm^2 in 12-well plates, and 24 h later (day 0) bPTH(1–34) was added at the concentrations indicated. In some wells, complete medium was replaced by serum-free medium on day 0 (No Serum). Random fields of cells were counted at 24-h intervals, and the *bars* indicate the SEM of triplicate determinations.

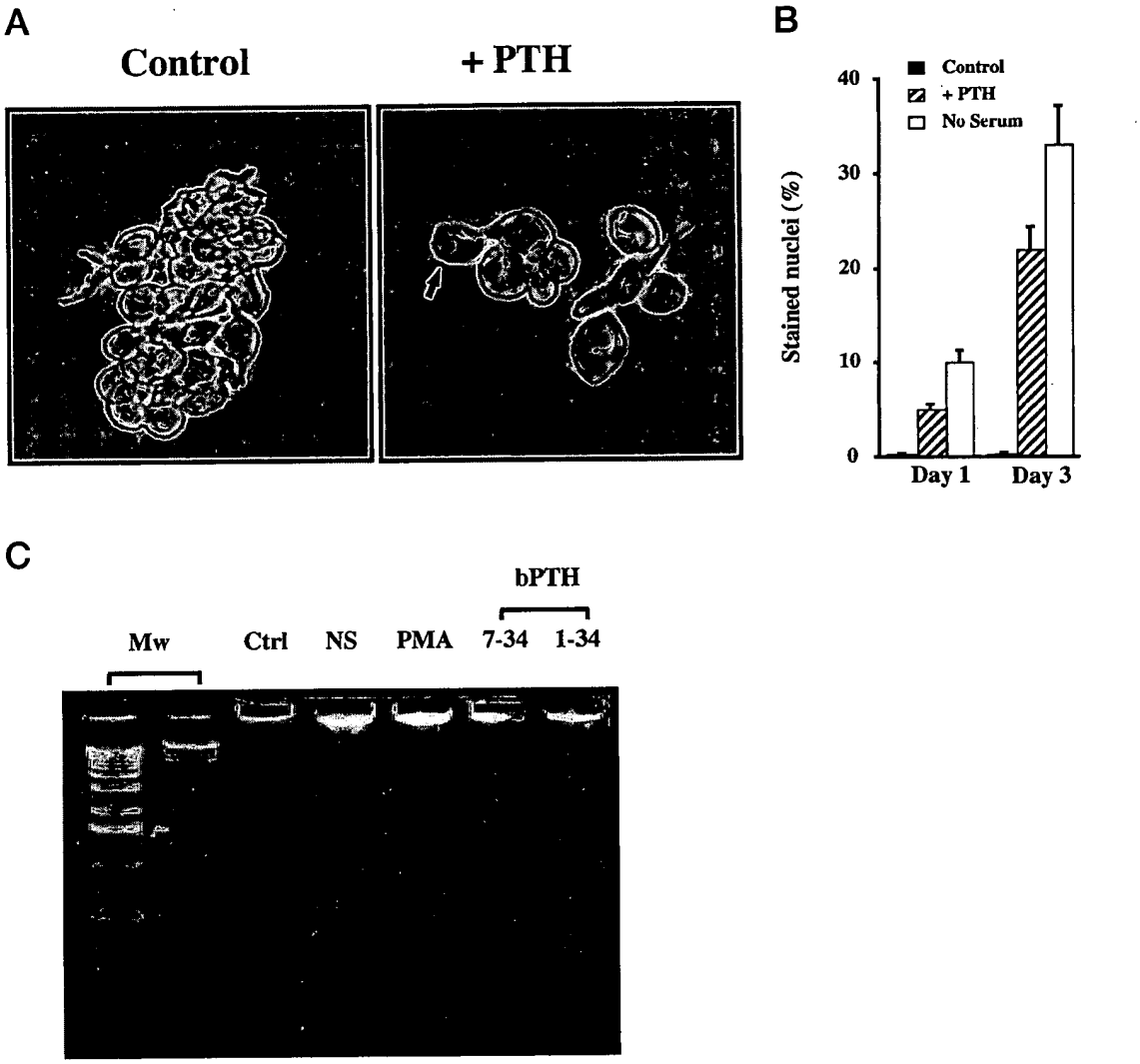

Fig. 2. Effects of bPTH(1–34) on Apoptosis of HEK 293 Cells Expressing the Wt PTHR

A, Apoptag staining of cells treated with or without bPTH(1–34) (1 μM) for 72 h. Positive peroxidase staining (*brown*) results from the labeling of DNA terminal fragments. B, Quantitation of TUNEL staining of 293 cells treated with or without bPTH(1–34) (1 μM) for 1 or 3 days, or after serum withdrawal for 3 days. All cells (including floating cells) were harvested and fixed before staining. Several hundred cells were counted for each data point: cells with *brown* staining were scored as positive, *blue* cells were scored as negative. Control cells at days 1 and 3 revealed less than 1% positive (apoptotic) staining. C, Agarose gel electrophoresis of DNA isolated from cells treated for 3 days in the following ways: maintained in the continuous presence of serum-containing medium (Ctrl); subject to serum withdrawal (NS); or exposed to PMA (400 nM), 1 μM bPTH(7–34) (a PTHR antagonist), or 1 μM bPTH(1–34).

tween these morphological changes and the apoptotic response to PTH is unclear.

DNA fragmentation is one of the final cellular events after exposure of cells to apoptotic stimuli (16). An earlier indicator of the activation of apoptosis pathways is the translocation of phosphatidylserine from the cytosolic to the extracellular face of the plasma membrane (17). This translocation can be monitored due to the high affinity of annexin V for phosphatidylserine. PTH treatment or serum withdrawal induced phoshatidylserine translocation to the extracellular plasma membrane surface within 5 h. The percent annexin V-stained cells increased from 3.6 ± 1.8% to 19.6 ± 4.1% after 5 h of exposure to bPTH(1–34) (1 μM) and to 44.7 ± 4.5% 5 h after serum withdrawal.

Characteristic nuclear changes are known to occur in response to apoptotic stimuli, including nuclear condensation and fragmentation (15). Hoechst 33342 nuclear dye staining revealed increased nuclear condensation and fragmentation of the nucleus in response to bPTH(1–34) or serum withdrawal, whereas heat treatment (48 C, 2 h) resulted in swollen, distended nuclei, characteristic of necrosis (not shown). These nuclear changes were readily apparent in elec-

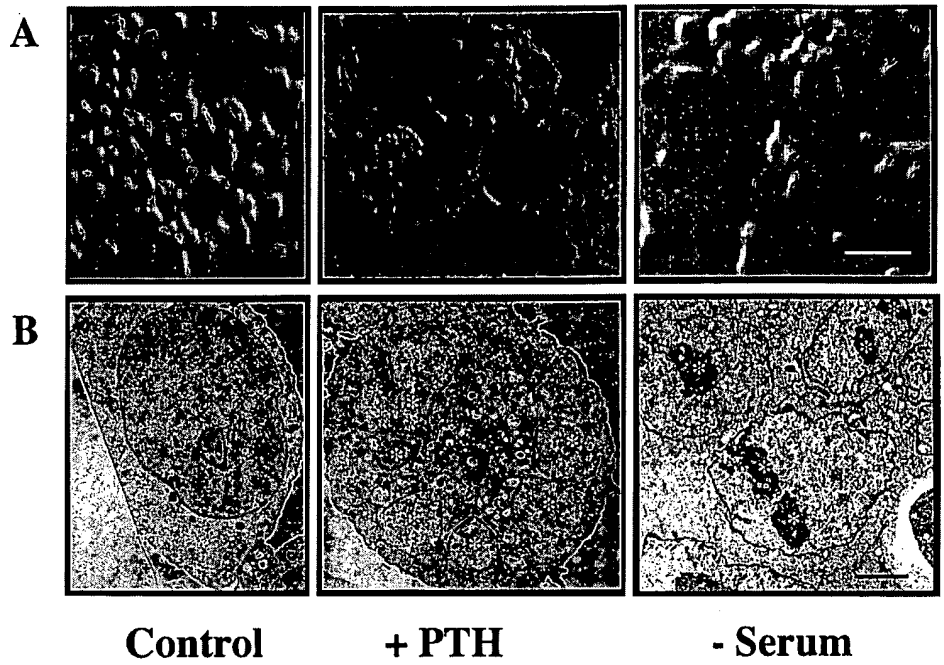

Fig. 3. Morphological Effects of PTH and Serum Withdrawal on HEK 293 Cells Expressing the Wt PTHR

A, Light microscope brightfield images 1 h after addition of normal growth media (control), 1 μM PTH(1–34), or 1 h after removal of serum. For all fields, the *white scale bar* = 25 μm. Cell flattening after PTH treatment and cell rounding and shrinkage after serum withdrawal were characteristically seen. B, Electron micrographs of cells grown as described in panel A. The nucleolus is visible in the center of the spherical control cell nucleus. *White stars* mark fragments of the nucleus in the PTH-treated cell. Fragmented nuclei were not seen in images of control cells. Mitochondrial morphology also appears to be disrupted by PTH treatment. *White stars* mark the condensations of chromatin visible in nuclei from cells subject to serum withdrawal. Ruffling of the nuclear membrane was also apparent in these cells, and whole-cell shrinkage was apparent. *White scale bars* = 2.5 μm.

tron micrographs of 293 cells after PTH treatment (Fig. 3C). Such fragmentation of the nucleus was not seen in any of more than 400 control cells that were examined. Cell fragmentation was also evident in electron micrographs after PTH treatment or serum deprivation (not shown). Such fragments most likely are a result of the final stages of apoptosis, which include loss of plasma membrane integrity and cytolysis. Cells undergoing these final stages of apoptosis could be visualized using a combination of a vital stain (Syto 13), together with propidium iodide (18). These dyes revealed a progressive loss of membrane integrity in response to both PTH and serum withdrawal, with a time course similar to that seen for DNA fragmentation (not shown).

The downstream effectors of mammalian apoptosis pathways are thought to be the caspase family of proteases (19). Preincubation of 293 cells for 3 h with cell-permeable inhibitors of caspases, YVAD (inhibitor of caspase 1), and DEVD (inhibitor of caspases 3, 8), significantly reduced the effects of PTH treatment on cell number (Fig. 4A) and apoptosis as determined by TUNEL (Fig. 4B). The amount of inhibitor used in each case was 0.2 μM, a dose known to be maximally effective in other systems (20, 21). The combination of both caspase inhibitors was more effective than either inhibitor alone, indicating that multiple caspases may participate in the apoptotic response. While the caspase inhibitors did not modify the suppressive effect of serum withdrawal on cell number, they did ameliorate the apoptotic response to serum withdrawal, indicating that serum contains essential growth factors that act independently of the apoptotic signaling pathway.

The oncogene product bcl-2 is known to inhibit apoptotic signaling in response to a wide range of stimuli. In 293 cells, bcl-2 is reported to partially inhibit apoptosis in response to serum deprivation (14). We evaluated 293 cells stably overexpressing bcl-2 as well as the Wt PTHR and found that bcl-2 partially prevented the effects of serum withdrawal on cell number and apoptosis (Fig. 5). However, overexpression of bcl-2 was ineffective in inhibiting the corresponding effects of bPTH(1–34).

The PTHR is known to signal through both the adenylyl cyclase/cAMP and PLC/Ca_i^{2+}/PKC pathways. We therefore investigated the role of these pathways in mediating the effects of PTH on 293 cell number and apoptosis. cAMP is known to induce apoptosis in certain cells such as T cells (22). However, two lines of evidence indicate that this pathway is neither necessary nor sufficient to produce apoptosis in 293 cells. First, receptor-independent production of cAMP, induced by treatment with forskolin, did not affect cell

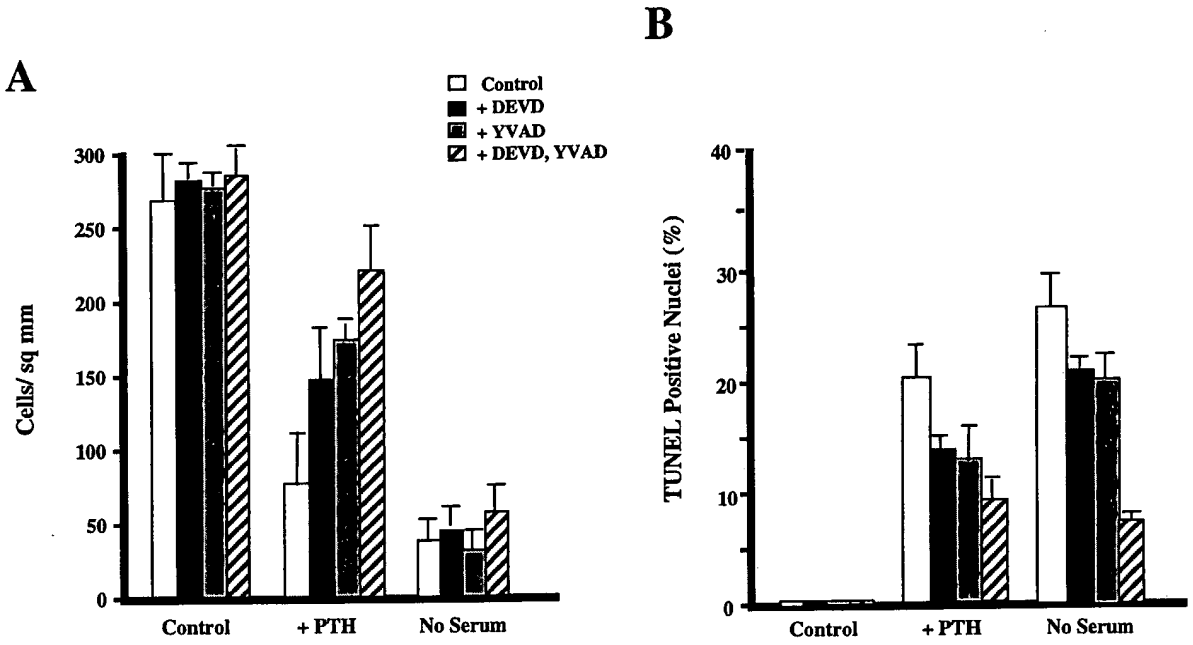

Fig. 4. Effect of Inhibitors of Caspase 1 (YVAD) or Caspases 3 and 8 (DEVD) on Growth Inhibition (A) and Apoptosis (B) of HEK 293 Cells after 3 Days of Serum Withdrawal (No Serum) or Treatment with bPTH(1–34) (1 μM)

Caspase inhibitors were added on day 0 and were present continuously (either separately or together) each at a concentration of 0.2 μM.

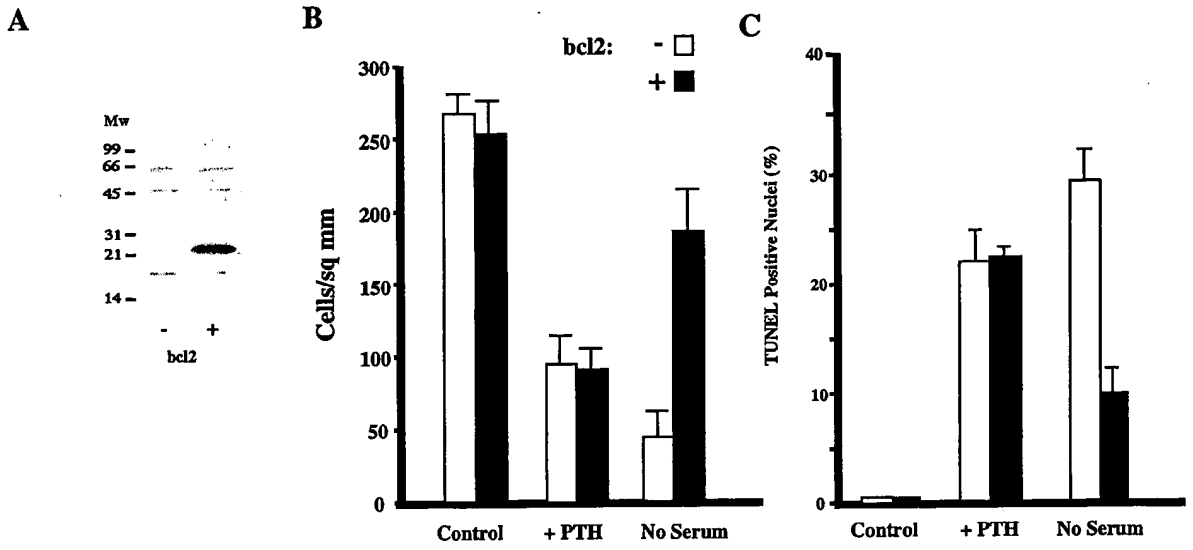

Fig. 5. Effect of Overexpression of bcl-2 on Cell Number and Apoptosis in HEK 293 Cells Treated with PTH or Subject to Serum Withdrawal

A, Western blot of bcl-2 in extracts of cells expressing the PTHR and bcl-2 (+), compared with cells expressing only the PTHR (−). The mobilities of the M_r markers are indicated. B, Effect of 3 days of treatment with bPTH(1–34) (1 μM) or 3 days of serum withdrawal on cell number in cells ± overexpression of bcl-2. C, Effect of 3 days of treatment with bPTH(1–34) (1 μM) or 3 days of serum withdrawal on apoptosis of cells ± overexpression of bcl-2.

number or induce apoptosis (Fig. 6). Second, activation of adenylyl cyclase via isoproteronol-induced activation of endogenous β_2-adrenergic receptors failed to reduce cell number or induce apoptosis (Fig. 6). β_2-Adrenergic receptors are known to signal via Gs-mediated activation of adenylyl cyclase, and not via Gq-mediated PKC/PLC activation. Third, 30 μM H-89, a concentration known to inhibit PKA in 293 cells (23),

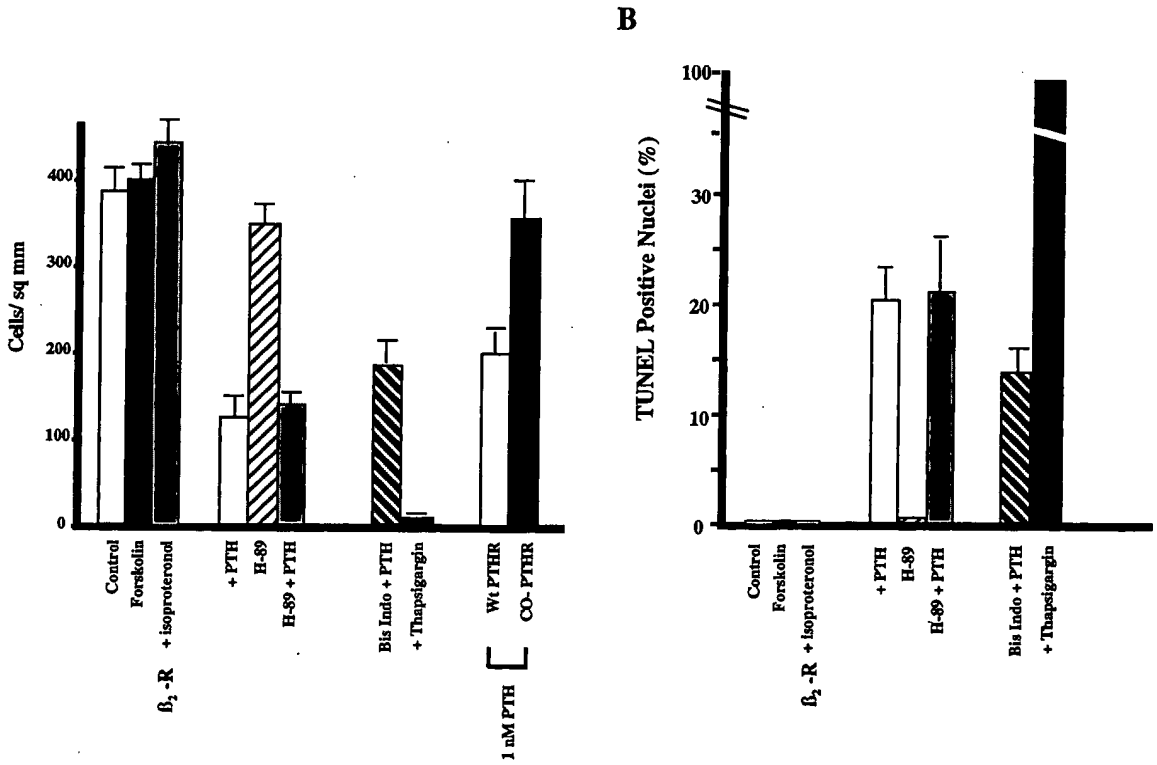

Fig. 6. Effects of Activators and Inhibitors of Signal Transduction Pathways on Cell Number (A) and Apoptosis (B) of HEK 293 Cells

Cells expressing the Wt PTHR were treated with forskolin (100 μM), the PKA inhibitor H-89 (30 μM), the PKC inhibitor GF 109203X (6 μM) (Bis Indo), or thapsigargin (0.4 nM). In some cases, cells were exposed to bPTH(1–34) (1 μM) for 3 days in the presence or absence of pharmacological agents. Cell number and apoptosis were also evaluated in HEK 293 cells overexpressing the β_2-adrenergic receptor (β_2-R) after a 3-day treatment with isoproterenol (10 μM). In panel A), the Wt and PLC-deficient PTHR (C0) were compared with respect to reduction in cell number in response to a submaximal dose of bPTH(1–34) (1 nM).

had no significant effect on PTH suppression of cell number or PTH-induced apoptosis (Fig. 6).

The other major signaling pathway activated by the PTHR is the Gq-mediated PLC/Ca_i^{2+}/PKC pathway. Several approaches were used to assess a possible role for this pathway in mediating the effects of PTH on cell number and apoptosis. Thapsigargin is a Ca^{2+}ATPase inhibitor that elevates intracellular calcium concentration $[Ca^{2+}]_i$, by promoting its release from intracellular stores, and induces apoptosis in certain cells (24). Thapsigargin was potent in reducing 293 cell number and inducing apoptosis (Fig. 6). The bisindolylmaleimide inhibitor of PKC, GF 109203X, at a maximally effective dose (6 μM) weakly inhibited (by ~20%) PTH-induced TUNEL staining, suggesting a minor role for PKC in the apoptotic response (Fig. 6B). Further support for a role for PLC came from the use of a mutant PTHR defective in PLC signaling. We have previously shown that alanine mutations of key residues in the N-terminal region of the third cytoplasmic loop of the PTHR (R377A,V378A, L379A), result in a receptor (termed C0) that displays reduced PTH-stimulated PLC signaling with retention of adenylyl cyclase signaling (25). Compared with 293 cells expressing the Wt PTHR, cell expressing this mutant were not as susceptible to the reduction in cell number elicited by a submaximal dose of bPTH(1–34) (1 nM) (Fig. 6A). At a maximal dose, however, bPTH(1–34) (1 μM) reduced cell number to the same degree as with cells expressing the Wt PTHR (data not shown). Further evidence for a role of PLC/Ca^{2+} signaling came from studies of 293 cells stably expressing the calcium-binding protein, calbindin-D28k. These cells were partially protected from both the reduction in cell number and the induction of apoptosis in response to PTH treatment (Fig. 7). However, calbindin overexpression did not protect cells from the effects of serum withdrawal.

To more precisely assess the role of specific G protein subunits in mediating the apoptotic action of PTH, we used 293 cells transfected with constructs encoding known inhibitors of $\beta\gamma$- and α_q-subunit function. RGS4 accelerates the GTPase activity of α_q and thereby inhibits receptor-mediated activation of effectors such PLC. A line of 293 cells stably overexpressing RGS4 has previously been shown to display suppressed receptor-stimulated PLC activity (26). We expressed the PTHR in these cells (which were kindly provided to us by Dr. Susanne Mumby), and assessed

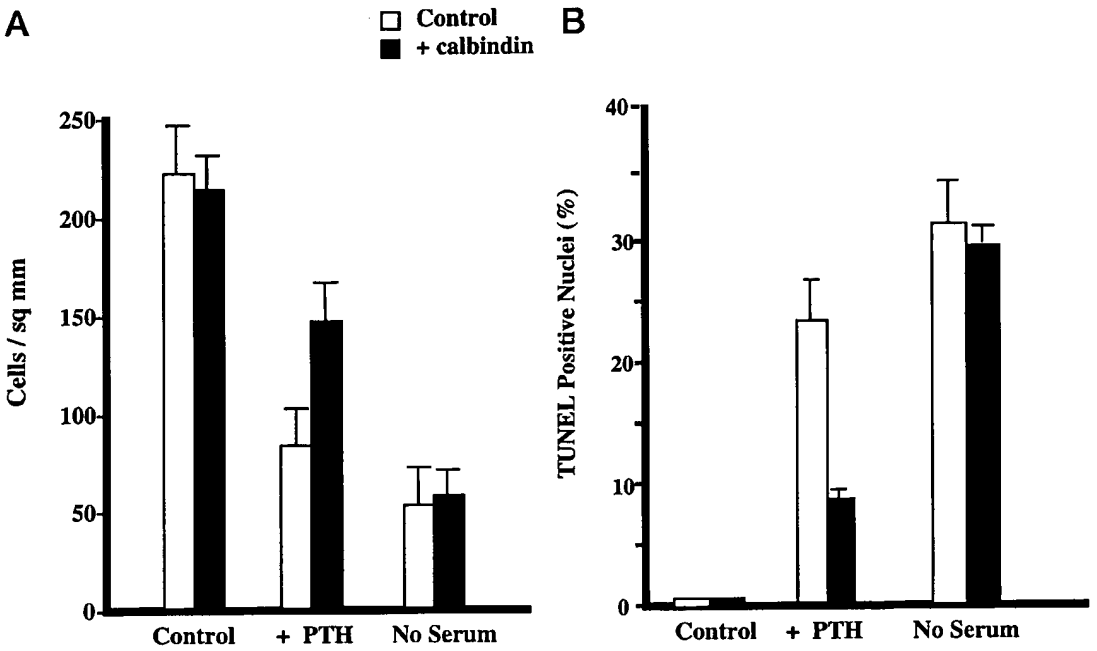

Fig. 7. Effect of bPTH(1–34) (1 μM) and Serum Withdrawal on Cell Number (A) and Apoptosis (B) of HEK 293 Cells Expressing the Wt PTHR with and without Overexpression of the Calcium-Binding Protein Calbindin

Cells were subject to PTH treatment (+ PTH) or serum withdrawal (No Serum) for 3 days. PTH-induced reduction in cell number and induction of apoptosis were significantly suppressed in cells overexpressing calbindin (P values <0.05 and <0.01, respectively).

the ability of PTH to produce a reduction in cell number and an increase in apoptosis (Fig. 8). Expression of RGS4 almost fully prevented the PTH-induced reduction in cell number and inhibited the apoptotic response to PTH by about 75%. A C-terminal fragment of G protein-coupled receptor kinase 2 (CtGRK2) is known to bind G protein $\beta\gamma$-subunits and thus to inhibit their ability to activate effectors (27). We evaluated the ability of the PTHR to initiate apoptotic signaling in 293 lines overexpressing CtGRK2 (Fig. 9). Overexpression of CtGRK2 blocked β-adrenergic receptor-mediated activation of MAP kinase, a process known to be dependent upon the $\beta\gamma$-subunits of Gi (28). This demonstrates that sufficient CtGRK2 was expressed to inhibit the functional activity of $\beta\gamma$-subunits after G protein activation. However, these cells were fully responsive to PTH, both with respect to the reduction in cell number and induction of apoptosis.

The ability of PTHR signaling to efficiently kill 293 cells made it possible to select cells resistant to this action. To accomplish this, 293 cells expressing the Wt PTHR were exposed to the UV-sensitive chemical mutagen, trimethylpsoralen (TMP), together with UV irradiation (29). Cells were subsequently grown in the continual presence of 1 μM bPTH(1–34). All cells exposed only to the mutagen or only to UV irradiation died within 2 weeks in the presence of bPTH(1–34). However, cells resistant to the killing effect of PTH were present in cultures treated with both TMP and UV irradiation. Twenty four clonal lines of PTH-resistant cells were isolated, of which 22 were found to bind radiolabeled PTHrP at levels comparable to nonmutagenized cells. The effects of PTH on cell number and apoptosis in two mutagenized clonal cell lines are shown in Fig. 10. These cell lines displayed markedly reduced sensitivity to the effects of PTH, but were fully sensitive to the effects of serum withdrawal. For these two clonal lines, and indeed for all of the 24 PTH-resistant clones (not shown), serum withdrawal induced apoptosis (Fig. 11). Also shown is the effect of tumor necrosis factor-α (TNFα) (10 ng/ml) on cell number and apoptosis of these cells. Nonmutagenized 293 cells displayed both reduction of cell numbers and apoptosis in response to TNFα. However, the mutagenized, PTH-resistant clonal cell lines proved to be heterogeneous, with several (such as clone 19) displaying resistance to the effects of TNFα, whereas others (such as clone 22) remained fully sensitive to TNFα.

DISCUSSION

The elucidation of mammalian apoptosis pathways has lagged behind that of *Caenorhabditis elegans* and is only partially defined at present in one case, that of the FAS/TNF receptor family (30). This highlights the importance of understanding other apoptosis pathways. The objectives of the present study were to

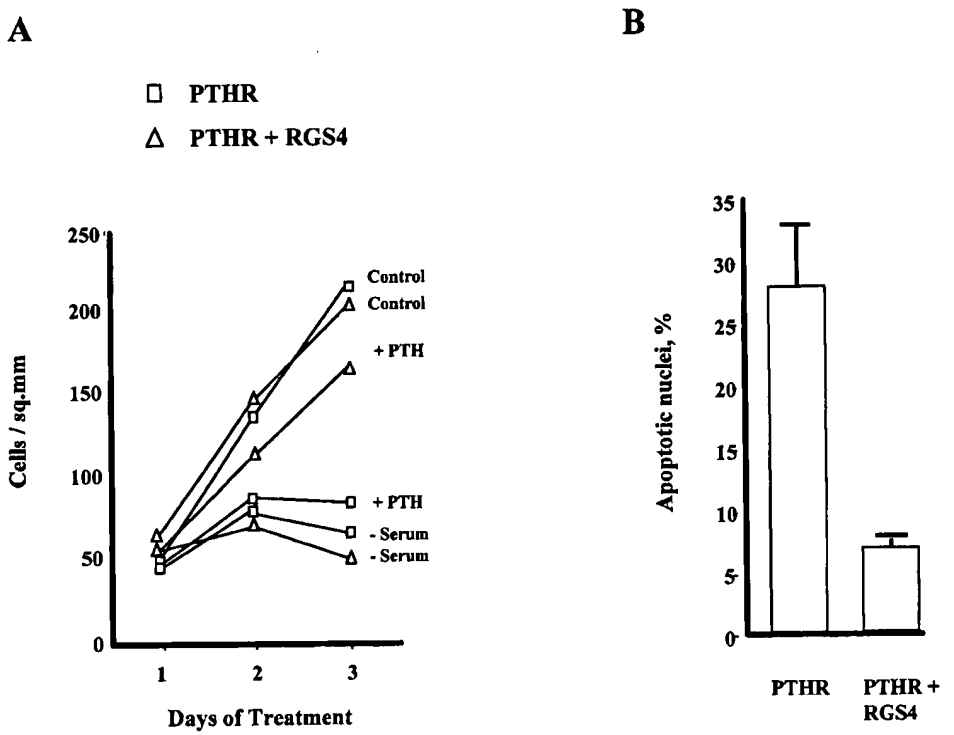

Fig. 8. Effects of RGS4 Expression on Cell Number (A) and Apoptosis (B) in HEK 293 Cells Expressing the Wt PTHR

A, Cells were maintained under normal growth conditions in the presence of serum (Control), treated with 1 μM bPTH(1–34) in the presence of serum (+ PTH), or grown in the absence of serum (–Serum). Daily counts of adherent cells were taken over a 3-day period. B, Cells were treated with 1 μM bPTH(1–34) for 3 days, and the percent of apoptotic nuclei was determined by TUNEL staining, as described in *Materials and Methods.* In both cases, cells expressing RGS4 were compared with cells stably transfected with the corresponding empty vector (pCB6).

assess whether PTHR activation can initiate apoptotic signaling and, if so, to characterize the signaling pathways mediating such a response.

Current understanding of mammalian apoptosis pathways is derived, in part, from the study of apoptosis induced by activation of the TNFα receptor (TNFR). Most cells express the TNFR (30), and TNFα was found in the present study to be a potent inducer of apoptosis in HEK293 cells (Fig. 10). Receptors in this TNFR superfamily contain a cytosolic region required for cell death signal transduction, termed the "death domain." After ligand binding and TNFR trimerization (Fig. 11), the death domain couples receptors to signaling molecules such as TRADD (TNFR-associated death domain protein). TRADD is an adapter molecule that couples receptors to caspase proteases. Recruitment of a procaspase to the receptor/TRADD complex results in procaspase cleavage and formation of an active dimer (20). The newly active caspase is then able to cleave various "death substrates" such as other caspases. More than 10 caspases have been identified thus far, and a variety of substrates have been characterized, including calpains, nuclear scaffold proteases, gelsolin, and signaling pathway components (19, 31). The end result of this caspase cascade is DNA fragmentation (19, 20) and the morphological criteria that distinguish apoptosis from necrosis such as DNA condensation and the fragmentation of the nucleus before cytolysis (18).

Evaluation of the amino acid sequence of the PTHR does not reveal the presence of a cytosolic death domain, indicating that an alternative mechanism likely to involve G protein activation initiates the apoptotic response to PTHR activation. PTHR-mediated apoptosis, like that induced by the TNFR, appears to require the activation of caspases, since apoptosis was partially abrogated by caspase inhibitors. That the inhibition was only partial may reflect the fact that other caspases in the cascade were activated or that inhibition of the caspases was incomplete. The combination of inhibitors was more effective than each inhibitor individually, consistent with the notion that PTHR-induced apoptosis is associated with the activation of multiple caspases. PTHR activation induced DNA fragmentation, as did serum withdrawal. Addition of PTH potentiated the effects of serum withdrawal (data not shown), a result that suggests that 293 cells possess at least two separate pathways by which apoptosis can be induced. In addition, PTH treatment induced other markers of apoptosis such as phosphatidyl serine translocation at an early time (5 h), and the number of cells with fragmented nuclei and lost

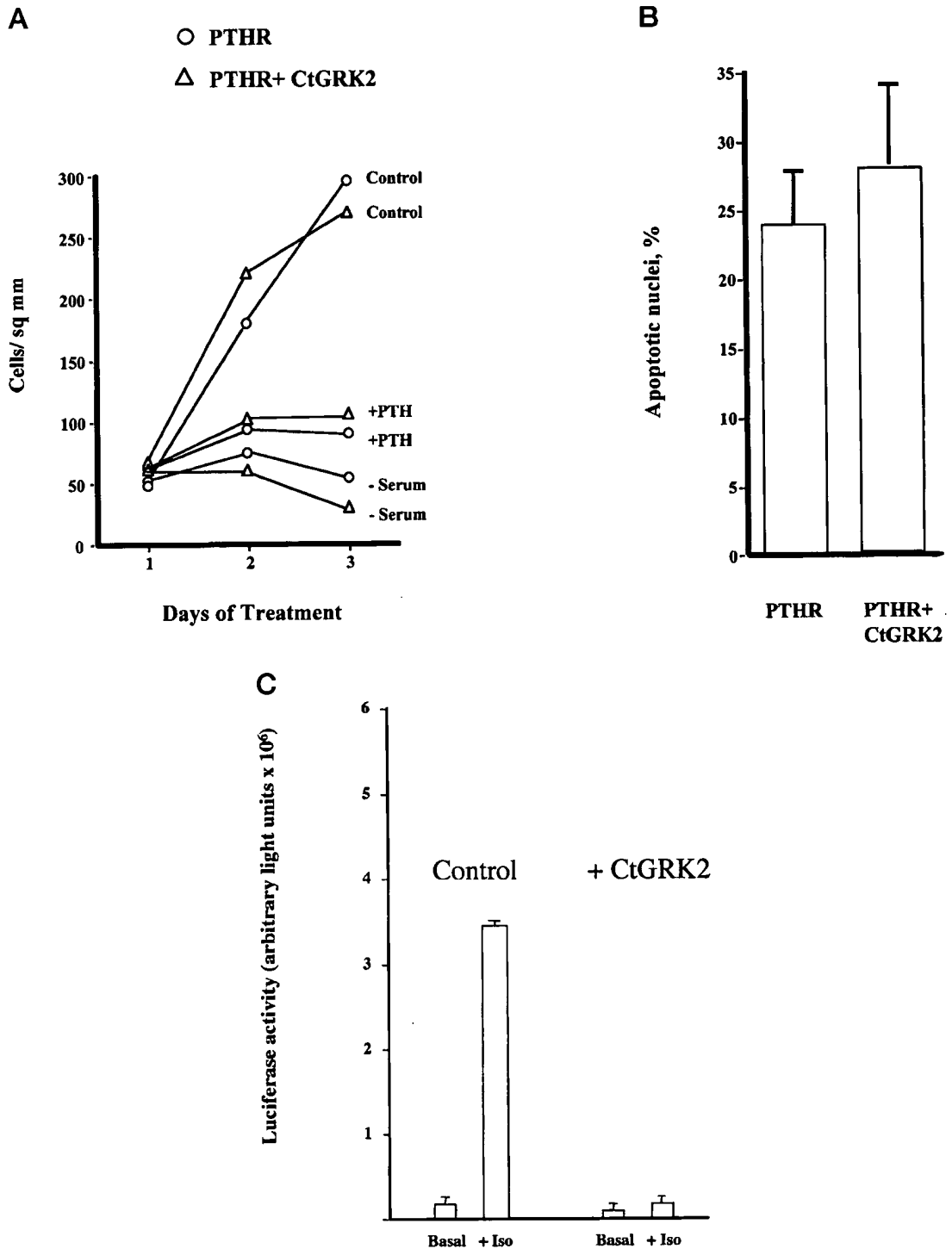

Fig. 9. Effects of CtGRK2 Expression on Cell Number (A), Apoptosis (B), and MAP Kinase (C) in HEK 293 Cells Expressing the Wt PTHR

A, Cells were maintained under normal growth conditions in the presence of serum (Control), treated with 1 μM bPTH(1–34) in the presence of serum (+ PTH), or grown in the absence of serum (−Serum). Daily counts of adherent cells were taken over a 3-day period. B, Cells were treated with 1 μM bPTH(1–34) for 3 days, and the percent of apoptotic nuclei was determined by TUNEL staining, as described in *Materials and Methods*. (C) Cells were transfected with a MAP kinase-activated luciferase reporter plasmid, as described in *Material and Methods*. Three days later, cells were treated with 1 μM isoproterenol, and luciferase activity was measured. In all three cases, cells expressing CtGRK2 were compared with cells transfected with the corresponding empty vector (pCEP4).

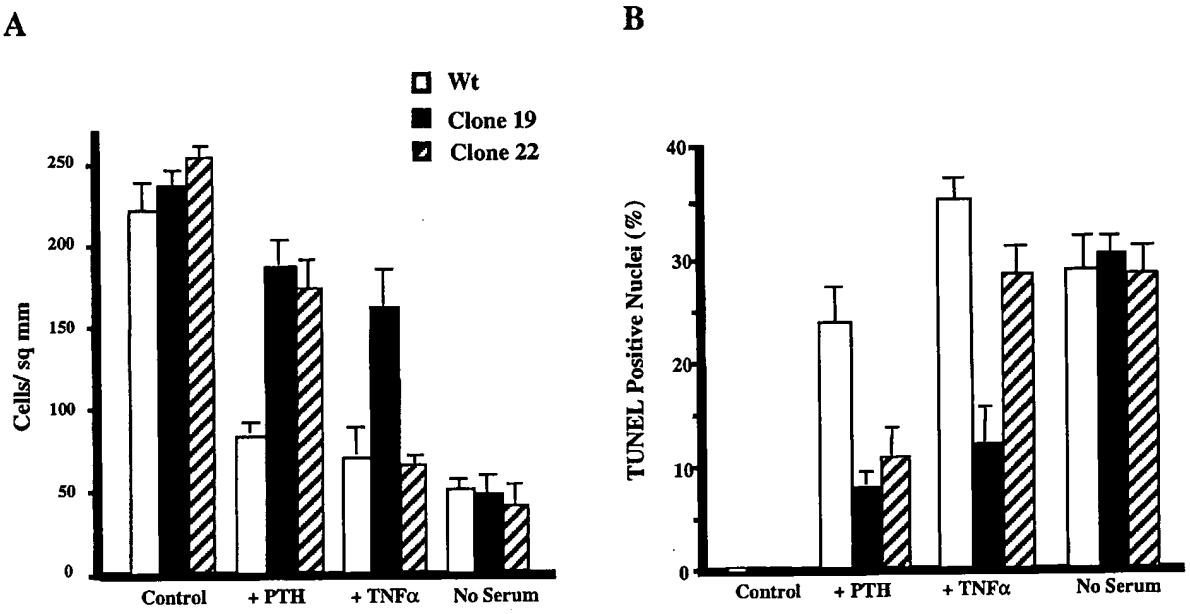

Fig. 10. Effects of PTH, TNFα, and Serum Withdrawal on Cell Number (A) and Apoptosis (B) of Control and Mutagen-Treated, PTH-Resistant Clonal HEK 293 Cells

Cells were treated with the mutagen TMP together with UV irradiation, and PTH-resistant clonal lines were isolated as described in *Materials and Methods*. Two PTH-resistant clonal lines were compared with non-mutagen-treated HEK cells expressing the Wt PTHR (Wt). Shown are the effects of 3 days of exposure to bPTH(1–34) (1 μM), TNFα (10 ng/ml), or serum withdrawal.

viability (assessed by electron or light microscopy) was similar to the number of cells with fragmented DNA as determined by TUNEL assay. These findings confirm that the effect of PTH on 293 cells was to induce apoptotic rather than necrotic cell death.

Mammalian cells can often be protected from apoptotic stimuli, including TNFα, by overexpression of the protooncogene bcl-2 (32). The mode of action of bcl-2 is at present unclear, although it may protect mitochondrial membrane integrity, prevent the pro-apoptotic activity of bcl-2 homologs such as bad or bax by forming inactive heterodimers (32), or perhaps act by inhibiting a protein required for caspase activation (33). Bcl-2 may exert its effect at the level of caspases 8 and 10, but it does not inhibit caspase 3, which may therefore be acting more downstream in the apoptosis cascade. In fact, bcl-2 can itself be a substrate for caspase 3 (34). Overexpression of bcl-2 has been found to repress transcription in response to serum withdrawal in 293 cells (14) and to abrogate serum withdrawal-induced apoptosis in PTHR expressing 293 cells (Fig. 5). However, bcl-2 overexpression did not prevent PTH-induced apoptosis, consistent with the utilization of a different pathway from that activated by serum withdrawal (Fig. 11). Thus, unlike the TNFR pathway, the PTHR-mediated apoptosis pathway appears to be bcl-2 independent. Alternately, it is possible that PTHR activation leads to a rapid degradation of bcl-2 even in cells overexpressing the protooncogene.

The PTHR-activated signaling pathway that induces apoptosis appears to be the Gq-mediated PLC/Ca_i^{2+} pathway. Increases in cAMP, known to induce apoptosis in certain cells (22), was neither necessary nor sufficient for PTH-induced apoptosis in 293 cells. PKC inhibition was only weakly effective at inhibiting PTH-induced cell death, suggesting a small contribution of PKC activation to apoptotic signaling, as has been observed in other systems (35). Thapsigargin was a powerful inducer of apoptosis, consistent with a role for calcium mobilization. A variety of studies have implicated changes in calcium ion homeostasis in apoptosis (36–39), but the underlying mechanisms are unclear. Experimentally induced calcium store depletion induced by stimulation of inositol-1,4,5- trisphosphate (IP_3) receptors or by inhibition of Ca^{2+}-ATPase activity can result in apoptosis (24, 40). It is possible that calcium store depletion is sensed by the cell and directly leads to an apoptotic response. Alternatively, it has been suggested that an increase in plasma membrane calcium permeability resulting from calcium store depletion signals apoptosis (41). Possible targets for the resulting elevations in $[Ca^{2+}]_i$ include proteases such as calpains or caspases, or protein kinases, which then promulgate the apoptotic signal (21). A crucial role for Ca_i^{2+} has been documented in neuronal cells where overexpression of the calcium-binding protein calbindin 28 kDa was found to rescue cells from apoptosis (41, 42), pre-

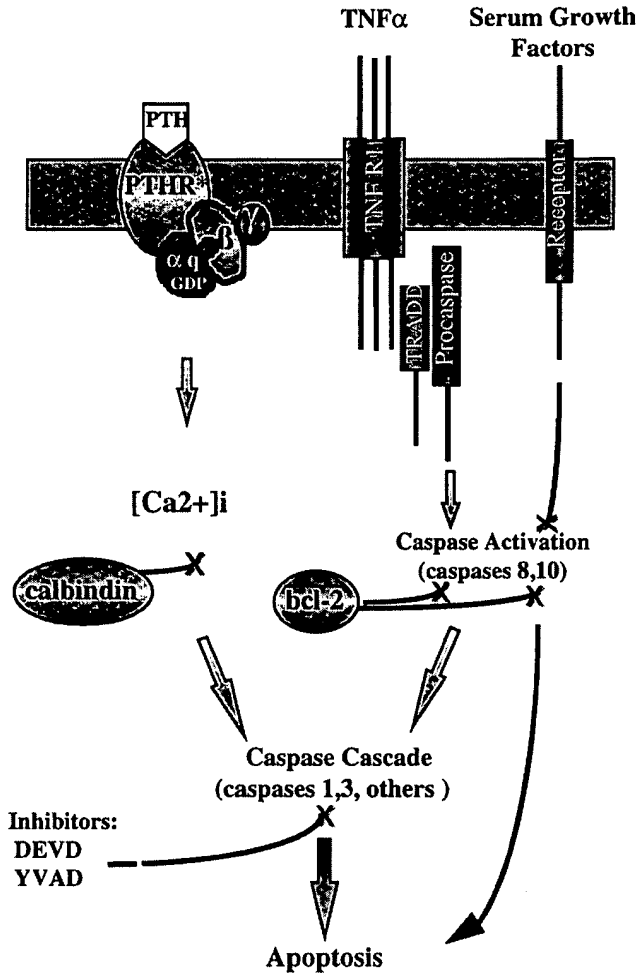

Fig. 11. Model Showing Putative Pathways Leading to Apoptosis Induced by PTHR Activation, TNFα, and Serum Withdrawal in HEK 293 Cells

For the PTHR, binding of PTH at the cell surface results in activation of Gs and Gq. The present results suggest that apoptosis is induced by an increase in $[Ca^{2+}]_i$ (which can be inhibited by calbindin D28K), presumably resulting from PLC activation mediated by the 34 α-subunit of Gq. Increased $[Ca^{2+}]_i$ induces apoptosis via activation of components of the caspase cascade, including caspases 1 and 3. Results from other studies indicate that activated TNFα receptors (TNFR1) recruit TRADD to the membrane, which in turn initiates a caspase cascade involving caspases 8 and 10 as well as caspases 1 and 3. Serum deprivation also produces activation of these caspases, leading ultimately to apoptosis. Bcl-2 is thought to act as an inhibitor of caspases 8 and 10, and thus protects cells from apoptosis induced by TNFα and serum withdrawal, but not PTH. Inhibitors of caspases 1 and 3 only partially protect cells from apoptosis, suggesting the existence of alternative downstream apoptotic pathways.

sumably by buffering the cytosol against increases in $[Ca^{2+}]_i$. In the present study, calbindin overexpression was found to protect 293 cells from PTH-induced apoptosis, but not from serum withdrawal-induced apoptosis. This supports the hypothesis that a PLC-dependent increase in $[Ca^{2+}]_i$ mediates PTHR-induced apoptosis, whereas the effect of serum withdrawal is independent of $[Ca^{2+}]_i$.

Of the two G protein pathways known to be activated by the PTHR, only G_q is affected by RGS4. Thus the observation that RGS4 markedly suppressed PTH-induced apoptosis strongly supports a role of G_q signaling in mediating the apoptotic response to PTH. Although the βγ-subunits of G_s or G_q that are released after PTHR activation could theoretically contribute to PLC activation (43), the finding that overexpression of CtGRK2 failed to inhibit apoptosis points to the central role of the α-subunit of G_q in initiating apoptotic signaling via PLC in this system.

The efficiency with which PTH treatment induced apoptosis of 293 cells expressing the Wt PTHR made it possible to use chemical mutagenesis with TMP together with UV irradiation to generate clonal cell lines resistant to this effect of PTH. Nearly all of the PTH-resistant clonal lines obtained displayed near Wt levels of PTHrP binding, ruling out loss of expression of the PTHR as the basis of PTH resistance in these lines. All of the PTH-resistant cell lines displayed ap-

optosis in response to serum withdrawal, indicating that downstream components of the apoptotic signaling pathway were intact. Some of the clonal lines also remained responsive to apoptosis induced by treatment with TNFα, suggesting that disruption of apoptotic signaling occurred relatively upstream in the PTHR-mediated apoptotic pathway (*e.g.* at the level of phospholipase C activation or Ca_i^{2+} mobilization/action) (Fig. 11). Other cell lines were resistant to TNFα as well as PTH, indicating that TMP/UV-induced disruption occurs at more distal sites that are common to the actions of both agents (*e.g.* at the level of the caspase cascade. These PTH-resistant cell lines will be helpful in defining the nature of the apoptotic signaling pathways used by PTH and TNFα.

In conclusion, these results indicate that PTHR signaling elicits an apoptotic response in 293 cells by a mechanism other than activation of adenylyl cyclase. The present study provides evidence that apoptosis is mediated by the Gq-PLC/Ca_i^{2+} signaling pathway. The apoptosis so produced differs from that induced by serum withdrawal in that bcl-2 does not protect against PTHR activation, whereas calbindin overexpression protects against apoptosis elicited by PTH, but not serum withdrawal. In addition, the PTHR and TNFR pathways appear to share downstream components of apoptotic signaling. Thus, this model system will be useful in the further characterization of the molecular mechanisms of PTH-induced apoptosis and in the identification of novel components of the PTHR-mediated apoptotic signaling pathway. Additional studies are in progress to assess the relevance of the apoptotic signaling pathway identified here to the diverse physiological responses initiated by the PTHR *in vivo*.

MATERIALS AND METHODS

Materials

Synthetic bPTH(1–34) and bPTH(7–34) were from Bachem California, Inc. (Torrance, CA). TNFα was obtained from R&D systems (Minneapolis, MN). The apoptag (TUNEL) assay kit was from Oncor (Gaithersburg, MD). Enhanced green fluorescent protein (EGFP), Annexin V Kit, and cell-permeable caspase inhibitors zYVAD and zDEVD were obtained from CLONTECH Laboratories, Inc. (Palo Alto, CA). Hoechst 33342 nuclear dye, TMP, methylgreen, forskolin, H-89, the bisindolylmaleidmide GF 109203X, and paraformaldehyde were obtained from Sigma (St. Louis, MO). Syto 13 vital dye was obtained from Calbiochem (San Diego, CA). Thapsigargin was obtained from Molecular Probes, Inc. (Eugene, OR). The monoclonal antibody against bcl-2 was from Santa Cruz Biotechnology, Inc. (Santa Cruz, CA).

Stable Cell Lines

HEK 293 cells were transfected with the cDNA encoding the opossum kidney (OKO) PTH receptor (kindly provided by Drs. H. Jüppner and G. Segre). subcloned into pCDNA3.1 (Invitrogen, Carlsbad, CA). After transfection using the Ca_2PO_4 precipitation method (44), clones were selected with G418 antibiotic (200 μg/ml) and isolated using limiting dilution in 96 well plates. Receptor expression was confirmed using Western blotting and ligand binding (^{125}I-PTHrP) techniques, as previously described (23). Complementary DNA encoding the human β_2-adrenergic receptor (kindly supplied by Dr. M. von Zastrow) was subcloned into the *Hin*dIII and *Not*I sites of the episomal vector pCEP4 (Invitrogen). Transfected cell pools were isolated by selecting cells in the presence of 200 μg/ml hygromycin. Control 293 cells were selected after transfection with pCEP4 vector alone. Complementary DNA encoding human bcl-2 (kindly supplied by Dr. S. Massa) and the C-terminal fragment of GRK2 (CtGRK2, kindly supplied by Dr. R. Lefkowitz) were subcloned into pCEP4; the rat calbindin 28 kDa cDNA was in pREP4 (45). Each construct was transfected separately into 293 cells stably expressing the PTHR, and hygromycin selection was carried out to generate transfected cell pools, as described above. cDNAs encoding the OKO Wt and the mutant PTH receptor R377A,V378A, L379A (C0) (25) were also subcloned into pCEP4 at the *Hin*dIII and *Not*I sites. These cDNAs were transfected into 293 cells, and selection was carried out with hygromycin as described above. Scatchard analysis demonstrated that the 293 cells lines expressed comparable numbers of Wt and mutant (C0) receptors (~500,000 receptors per cell). For studies of RGS4, 293 cells stably transfected with a cDNA encoding RGS4 (in the expression plasmid pCB6), and control cells stably transfected with pCB6 alone, were provided by Dr. S. Mumby (26). Each of these cell lines was transfected with a cDNA encoding the Wt PTHR in pCEP4, and selection of cell pools was carried out with hygromycin as described above. Comparable levels of functional PTHR expression were obtained in these cell lines.

Assessment of Cell Number

HEK 293 cells expressing the appropriate receptors were subcultured using 0.25% trypsin, and plated at a density of approximately 10^4 cells per well (50 cells/mm^2 in 12-well plates). Twenty four hours later, the medium (DMEM with 10% FCS, 1% penicillin/streptomycin) was replaced with medium containing PTH or with serum-free medium (t = 0) and cells were cultured for a 72-h period. Adherent cells were counted every 24 h. Cells did not approach confluence under these conditions.

TUNEL Assay

After 24, 48, and 72 h in culture, cells were detached using Ca^{2+}/Mg^{2+} free PBS. Cells were centrifuged at 300 rpm, the supernatant was removed, and cells were suspended and immediately fixed in 4% paraformaldehyde for 10 min. Aliquots of fixed cells were allowed to dry on a coverslip surface, and then washed in 10 mM Tris-HCl, pH 8.0, for 5 min. Cells were permeabilized with 0.1% Triton X-100 in 10 mM Tris-HCl, pH 8.0, for 5 min, and after washing with 10 mM Tris-HCl, pH 8.0, were preincubated with terminal deoxynucleotidyl transferase. After 10 min, the reaction mixture containing terminal deoxynucleotidyl transferase and biotinylated dUTP was added. After 1 h at 37 C, the reaction was terminated. Cells were washed with PBS and incubated with streptavidin peroxidase for 30 min. After extensive washing and counterstaining with methyl green, cells were examined and scored positive or negative for DNA fragmentation.

DNA Fragmentation by Gel Electrophoresis

293 cells in 10-cm dishes were lysed with 0.1 M NaCl, 10 mM Tris HCl, pH 7.4, and 1 mM EDTA with 0.3% SDS, and incubated with proteinase K overnight at 55 C. Samples were extracted with phenol/chloroform, and DNA was precipitated and resuspended in Tris-EDTA, pH 8.0, and treated with ribonuclease for 1 h at 37 C. Electrophoresis was performed

on a 4% agarose gel at 50 V for 4 h, in the presence of 0.5 μg/ml ethidium bromide.

Evaluation of MAP Kinase Activation

β-Adrenergic stimulation of MAP kinase was assessed using an Elk1 reporter system (PathDetect, Stratagene). In brief, 293 cells stably expressing the Wt PTHR were cotransfected (using the calcium phosphate method) with two plasmids – one encoding the transactivation domain of Elk1 (fused to the DNA-binding domain of GAL4) and other containing a luciferase reporter gene bearing tandem repeats of a GAL4 binding sequence. Three days later, cells were treated ± 1 μM isoproterenol for 6 h, and luciferase activity was measured using the Promega Corp. luciferase assay kit according to the manufacturer's instructions.

Light/Fluorescence Microscopy

Light and fluorescence microscopy was carried out with an inverted Nikon (Garden City, NY) fluorescent microscope, equipped with 10×, 20×, and 40× objectives. For Annexin V staining, vital stain Syto 13, and propidium iodide, a fluorescein isothiocyanate/rhodamine filter set, was used. For Hoechst 33342 nuclear stain, a 340-nm excitation filter was used, and for EGFP visualization fluorescent excitation was carried out at 390 nm and a 510-nm emission filter was used.

Electron Microscopy

After 24, 48, and 72 h growth in 10-cm culture dishes, 293 cells were fixed with 2.5% glutaraldehyde in ice-cold 0.2 M sodium cacodylate buffer (pH 7.4) for 4 h. Cells were washed in PBS three times and postfixed in 1% osmium tetroxide for 30 min. Cells were then dehydrated in ascending grades of ethyl alcohol and embedded in resin. Ultrathin sections were cut and stained with uranyl acetate and lead citrate (4%) and examined using a H7000 electron microscope (Hitachi Scientific Instruments, Inc., San Jose, CA).

TMP Mutagenesis

A 3 mg/ml stock solution of TMP in dimethylsulfoxide was diluted with DMEM to a final concentration of 30 μg/ml. This TMP solution was added to 293 cells expressing the Wt PTHR, and the flasks were rocked in the dark for 15 min at room temperature. Cells were then exposed to UV irradiation (Blak-Ray lamp, 350 $\mu W/cm^2$, Fisher Scientific, Pittsburgh, PA) for 60 sec. Cells were allowed to grow for 16 h at 37 C, after which time 1 μM bPTH(1–34) was added to the medium. Subsequently, cells were grown in the continuous presence of bPTH(1–34) until all cells died or until surviving clones were of sufficient size to isolate using a cloning ring (~14 days after UV treatment). These PTH-resistant cells were expanded for further study.

Acknowledgments

Received December 28, 1998. Re-revision received October 14, 1999. Accepted October 18, 1999.

Address requests for reprints to: Robert A. Nissenson, Ph.D., Endocrine Unit, Veterans Affairs Medical Center (111N), 4150 Clement Street, San Francisco, California 94121. E-mail: chicago@itsa.ucsf.edu.

This work was supported by funds from the Medical Research Service of the Department of Veterans' Affairs (R.A.N.), by NIH Grant DK-35323 (R.A.N), and by a Research Evaluation and Allocation Committee award from University of California San Francisco (P.R.T.). Dr. Nissenson is a Research Career Scientist of the Department of Veterans' Affairs.

REFERENCES

1. Amling M, Neff L, Tanaka S, Inoue D, Kuida K, Weir E, Philbrick WM, Broadus AE, Baron R 1997 Bcl-2 lies downstream of parathyroid hormone-related peptide in a signaling pathway that regulates chondrocyte maturation during skeletal development. J Cell Biol 136:205–213
2. Yang XLJ, Wolfe J, Cain RL, Onyia JE, Santerre RF, Hock JM 1997 Selective stimulation of apoptosis in trabecular osteoblasts and osteocytes of young rats treated with once daily hPTH 1–34 to increase bone mass. J Bone Miner Res 12[Suppl 1]:S316
3. Kano J, Sugimoto T, Kanatani M, Kuroki Y, Tsukamoto T, Fukase M, Chihara K 1994 Second messenger signaling of c-fos gene induction by parathyroid hormone (PTH) and PTH-related peptide in osteoblastic osteosarcoma cells: its role in osteoblast proliferation and osteoclast-like cell formation. J Cell Physiol 161:358–366
4. Sabatini M, Lesur C, Pacherie M, Pastoureau P, Kucharczyk N, Fauchère JL, Bonnet J 1996 Effects of parathyroid hormone and agonists of the adenylyl cyclase and protein kinase C pathways on bone cell proliferation. Bone 18:59–65
5. Onishi T, Hruska K 1997 Expression of p27Kip1 in osteoblast-like cells during differentiation with parathyroid hormone. Endocrinology 138:1995–2004
6. Jüppner H, Abou-Samra AB, Freeman M, Kong XF, Schipani E, Richards J, Kolakowski Jr LF, Hock J, Potts Jr JT, Kronenberg HM, Segre GV 1991 A G protein-linked receptor for parathyroid hormone and parathyroid hormone-related peptide. Science 254:1024–1026
7. Karaplis AC, Luz A, Glowacki J, Bronson RT, Tybulewicz VL, Kronenberg HM, Mulligan RC 1994 Lethal skeletal dysplasia from targeted disruption of the parathyroid hormone-related peptide gene. Genes Dev 8:277–289
8. Lanske B, Karaplis AC, Lee K, Luz A, Vortkamp A, Pirro A, Karperien M, Defize LHK, Ho C, Mulligan RC, Abou-Samra AB, Jüppner H, Segre GV, Kronenberg HM 1996 PTH/PTHrP receptor in early development and Indian hedgehog-regulated bone growth [see comments]. Science 273:663–666
9. Amizuka N, Warshawsky H, Henderson JE, Goltzman D, Karaplis AC 1994 Parathyroid hormone-related peptide-depleted mice show abnormal epiphyseal cartilage development and altered endochondral bone formation. J Cell Biol 126:1611–1623
10. Schipani E, Kruse K, Jüppner H 1995 A constitutively active mutant PTH-PTHrP receptor in Jansen-type metaphyseal chondrodysplasia. Science 268:98–100
11. Schipani E, Langman CB, Parfitt AM, Jensen GS, Kikuchi S, Kooh SW, Cole WG, Jüppner H 1996 Constitutively activated receptors for parathyroid hormone and parathyroid hormone-related peptide in Jansen's metaphyseal chondrodysplasia [see comments]. N Engl J Med 335:708–714
12. Vortkamp A, Lee K, Lanske B, Segre GV, Kronenberg HM, Tabin CJ 1996 Regulation of rate of cartilage differentiation by Indian hedgehog and PTH-related protein [see comments]. Science 273:613–622
13. Zenmyo M, Komiya S, Kawabata R, Sasaguri Y, Inoue A, Morimatsu M 1996 Morphological and biochemical evidence for apoptosis in the terminal hypertrophic chondrocytes of the growth plate. J Pathol 180:430–433
14. Grimm S, Bauer MK, Baeuerle PA, Schulze-Osthoff K 1996 Bcl-2 down-regulates the activity of transcription factor NF-κB induced upon apoptosis. J Cell Biol 134: 13–23

15. Allen RT, Hunter WJ, 3rd, Agrawal DK 1997 Morphological and biochemical characterization and analysis of apoptosis. J Pharmacol Toxicol Methods 37:215–228
16. Peter ME, Heufelder AE, Hengartner MO 1997 Advances in apoptosis research. Proc Natl Acad Sci USA 94: 12736–12737
17. Walton M, Sirimanne E, Reutelingsperger C, Williams C, Gluckman P, Dragunow M 1997 Annexin V labels apoptotic neurons following hypoxia-ischemia. Neuroreport 8:3871–3875
18. Eguchi Y, Shimizu S, Tsujimoto Y 1997 Intracellular ATP levels determine cell death fate by apoptosis or necrosis. Cancer Res 57:1835–1840
19. Salvesen GS, Dixit VM 1997 Caspases: intracellular signaling by proteolysis. Cell 91:443–446
20. Du Y, Bales KR, Dodel RC, Hamilton-Byrd E, Hom JW, Czilli DL, Simmons LK, Ni B, Paul SM 1997 Activation of a caspase 3-related cysteine protease is required for glutamate-mediated apoptosis of cultured cerebellar granule neurons. Proc Natl Acad Sci USA 94:11657–11662
21. Gressner AM, Lahme B, Roth S 1997 Attenuation of TGF-beta-induced apoptosis in primary cultures of hepatocytes by calpain inhibitors. Biochem Biophys Res Commun 231:457–462
22. Ivanov VN, Lee RK, Podack ER, Malek TR 1997 Regulation of Fas-dependent activation-induced T cell apoptosis by cAMP signaling: a potential role for transcription factor NF-κ B. Oncogene 14:2455–2464
23. Blind E, Bambino T, Nissenson RA 1995 Agonist-stimulated phosphorylation of the G protein-coupled receptor for parathyroid hormone (PTH) and PTH-related protein. Endocrinology 136:4271–4277
24. Lin XS, Denmeade SR, Cisek L, Isaacs JT 1997 Mechanism and role of growth arrest in programmed (apoptotic) death of prostatic cancer cells induced by thapsigargin. Prostate 33:201–207
25. Huang Z, Chen Y, Pratt S, Chen TH, Bambino T, Nissenson RA, Shoback DM 1996 The N-terminal region of the third intracellular loop of the parathyroid hormone (PTH)/PTH-related peptide receptor is critical for coupling to cAMP and inositol phosphate/Ca2+ signal transduction pathways. J Biol Chem 271:33382–33389
26. Huang C, Hepler JR, Gilman AG, Mumby SM 1997 Attenuation of Gi- and Gq-mediated signaling by expression of RGS4 or GAIP in mammalian cells. Proc Natl Acad Sci USA 94:6159–6163
27. Koch WJ, Hawes BE, Inglese J, Luttrell LM, Lefkowitz RJ 1994 Cellular expression of the carboxyl terminus of a G protein-coupled receptor kinase attenuates G beta gamma-mediated signaling. J Biol Chem 269:6193–6197
28. Daaka Y, Luttrell LM, Lefkowitz RJ 1997 Switching of the coupling of the beta2-adrenergic receptor to different G proteins by protein kinase A. Nature 390:88–91
29. Yandell MD, Edgar LG, Wood WB 1994 Trimethylpsoralen induces small deletion mutations in *Caenorhabditis elegans*. Proc Natl Acad Sci USA 91:1381–1385
30. Darnay BG, Aggarwal BB 1997 Early events in TNF signaling: a story of associations and dissociations. J Leukoc Biol 61:559–566
31. Widmann C, Gibson S, Johnson GL 1998 Caspase-dependent cleavage of signaling proteins during apoptosis. A turn-off mechanism for anti-apoptotic signals. J Biol Chem 273:7141–7147
32. Strasser A, Huang DC, Vaux DL 1997 The role of the bcl-2/ced-9 gene family in cancer and general implications of defects in cell death control for tumourigenesis and resistance to chemotherapy. Biochim Biophys Acta 1333:F151–178
33. Giambarella U, Yamatsuji T, Okamoto T, Matsui T, Ikezu T, Murayama Y, Levine MA, Katz A, Gautam N, Nishimoto I 1997 G protein βγ complex-mediated apoptosis by familial Alzheimer's disease mutant of APP. EMBO J 16:4897–4907
34. Grandgirard D, Studer E, Monney L, Belser T, Fellay I, Borner C, Michel MR 1998 Alphaviruses induce apoptosis in Bcl-2-overexpressing cells: evidence for a caspase-mediated, proteolytic inactivation of Bcl-2. EMBO J 17:1268–1278
35. Lucas M, Sánchez-Margalet V 1995 Protein kinase C involvement in apoptosis. Gen Pharmacol 26:881–887
36. Althoefer H, Eversole-Cire P, Simon MI 1997 Constitutively active Gαq and Gα13 trigger apoptosis through different pathways. J Biol Chem 272:24380–24386
37. Chattopadhyay N, Vassilev PM, Brown EM 1997 Calcium-sensing receptor: roles in and beyond systemic calcium homeostasis. Biol Chem 378:759–768
38. Furuya Y, Lundmo P, Short AD, Gill DL, Isaacs JT 1994 The role of calcium, pH, and cell proliferation in the programmed (apoptotic) death of androgen-independent prostatic cancer cells induced by thapsigargin. Cancer Res 54:6167–6175
39. McConkey DJ, Orrenius S 1997 The role of calcium in the regulation of apoptosis. Biochem Biophys Res Commun 239:357–366
40. Jayaraman T, Marks AR 1997 T cells deficient in inositol 1,4,5-trisphosphate receptor are resistant to apoptosis. Mol Cell Biol 17:3005–3012
41. Lee S, Christakos S, Small MB 1993 Apoptosis and signal transduction: clues to a molecular mechanism. Curr Opin Cell Biol 5:286–291
42. Mattson MP, Cheng B, Baldwin SA, Smith-Swintosky VL, Keller J, Geddes JW, Scheff SW, Christakos S 1995 Brain injury and tumor necrosis factors induce calbindin D-28 k in astrocytes: evidence for a cytoprotective response. J Neurosci Res 42:357–370
43. Katz A, Wu D, Simon MI 1992 Subunits β γ of heterotrimeric G protein activate β 2 isoform of phospholipase C. Nature 360:686–689
44. Chen C, Okayama H 1987 High-efficiency transformation of mammalian cells by plasmid DNA. Mol Cell Biol 7:2745–2752
45. Pollock AS, Santiesteban HL 1995 Calbindin expression in renal tubular epithelial cells. Altered sodium phosphate co-transport in association with cytoskeletal rearrangement. J Biol Chem 270:16291–16301